EFFECTS OF MEAN FLOW ON THE
DYNAMIC CHARACTERISTICS OF
FLUID TRANSMISSION LINES

THESIS

Mark S. Briski
First Lieutenant, USAF

AFIT/GAE/AA/83D-2

DEPARTMENT OF THE AIR FORCE
AIR UNIVERSITY
AIR FORCE INSTITUTE OF TECHNOLOGY

Wright-Patterson Air Force Base, Ohio

EFFECTS OF MEAN FLOW ON THE
DYNAMIC CHARACTERISTICS OF
FLUID TRANSMISSION LINES

THESIS

Mark S. Briski
First Lieutenant, USAF

AFIT/GAE/AA/83D-2

Approved for public release; distribution unlimited

AFIT/GAE/AA/83D-2

EFFECTS OF MEAN FLOW ON THE DYNAMIC CHARACTERISTICS OF FLUID TRANSMISSION LINES

THESIS

Presented to the Faculty of the School of Engineering

of the Air Force Institute of Technology

Air University

In Partial Fulfillment of the

Requirements for the Degree of

Master of Science in Aeronautical Engineering

Mark S. Briski, B.S.

First Lieutenant, USAF

December 1983

Approved for public release; distribution unlimited

Preface

The purpose of this thesis was to study the effects of turbulent mean flow on the frequency response of round air filled transmission lines. The report was based heavily on past theses and dissertations performed at the Air Force Institute of Technology, specifically those written by Malanowski, Vining, and Moore.

The computer program used in this study was originally written by Malanowski and the model used to predict turbulent characteristics was developed by Moore with modifications suggested by Dr. Franke.

I wish to thank the people who were helpful in the completion of this study. Captain Mark Ross devoted much on a thesis with a similar topic and was very helpful in almost all phases of this study. Dr. Milton Franke, my thesis advisor, was always helpful whenever I ran into problems. Harley Linville was always ready to help when equipment problems cropped up. I also wish to thank my wife, Theresa, for putting up with me during the final months of study and typing.

Mark S. Briski

Contents

List of Figures

List of Tables

List of Symbols

Symbol	Description	Units
A	line cross-sectional area	in^2
Beta	phase angle	radians
C	capacitance/unit length	$\frac{\text{cis-sec}}{\text{psi}}/\text{in}$
C_a	adiabatic capacitance/unit length; $A/\gamma P$ for ideal gas	$\frac{\text{cis-sec}}{\text{psi}}/\text{in}$
D	line diameter	in
f	friction factor	dimensionless
g	dynamic pressure ratio, P_r/P_s	dimensionless
g_{ct}	line gain	decibels
G	conductance/unit length	$\frac{\text{cis}}{\text{psi}}/\text{in}$
h_v	velocity distribution parameter	dimensionless
h_t	temperature distribution parameter	dimensionless
j	$\sqrt{-1}$	dimensionless
L	inertance/unit length	$\frac{\text{psi/sec}}{\text{cis}}/\text{in}$
L_a	adiabatic inertance/unit length ρ/A for ideal gas	$\frac{\text{psi/sec}}{\text{cis}}/\text{in}$
l	line length	in
$\bar{P}$	DC (mean) Pressure at beginning of the line	psi
P	AC pressure	psi
Q	volumetric flow rate (DC)	cis

Symbol	Description	Units
R	resistance/unit length	$\frac{psi}{cis}/in$
r	line radius	in
Re	Reynolds number based on diameter	dimensionless
R_g	real gas constant	$\frac{in^2}{sec^{2\,o}R}$
R_{v_T}	turbulent viscous resistance	$\frac{psi}{cis}/in$
R_{v_l}	laminar viscous resistance	$\frac{psi}{cis}/in$
T	temperature	^oR
$\bar{u}$	mean velocity	in/sec
x	distance downstream in line	in
Y	shunt admittance/unit length	$\frac{cis}{psi}/in$
Z	impedance/unit length	$\frac{psi}{cis}/in$
Z_c	characteristic impedance/unit length $\sqrt{Z/Y}$	psi/cis
Z_T	terminal or end impedance	psi/cis
α	attenuation/unit length	neper/in
β	phase shift/unit length	rad/in
Γ	propagation constant/unit length $\sqrt{ZY}$	1/in
γ	ratio of specific heats	dimensionless
μ	dynamic viscosity	psi-sec

Symbol	Description	Units
ν	kinematic viscosity	in^2/sec
ρ	density	$lb_f\text{-}sec^2/in^4$
σ	Prandtl number	dimensionless
Ω	non-dimensional frequency $r^2\omega/\nu$	dimensionless
Ω_b	non-dimensional break frequency	dimensionless
ω	angular frequency	rad/sec
$\omega_{b,DC}$	break frequency of model with DC resistance	rad/sec
$\omega_{b,AC}$	break frequency of model with AC resistance	rad/sec
ω_v	viscous characteristic frequency; $8\pi\nu/A$	rad/sec
ω_t	thermal characteristic frequency; ω_v/σ^2	rad/sec

Subscripts

a	adiabatic
A	absolute
r	recieving end properties
s	sending end properties
t	turbulent

Abstract

Theoretical predictions of the small signal frequency response of round pneumatic transmission lines with turbulent mean flow were compared with experimental results. The frequency response curves were found for lines varying in length from 24 to 36 in. with inside diameters of 0.195, 0.119, and 0.041 in. The lines were tested at Reyn numbers of 2000, 5000, and 10000.

Theoretical solutions were obtained using Nich equations as modified by Krishnaiyer and Lechner. Solutions were also found using several different modifications of a constant LRC model developed by Moore. The results were mixed: for the 0.195 and 0.119 in. lines the prediction of gain was good but for the 0.041 in. lines the results were poor. The accuracy and applicability of the constant LRC model was explored along with its various modifications. The constant LRC model with the AC resistance showed potential for predicting the gain in fluid transmission lines with turbulent flow. The limitations and applicability of the constant LRC models was studied.

THE EFFECTS OF MEAN FLOW ON THE DYNAMIC CHARACTERISTICS OF FLUID TRANSMISSION LINES

I. Introduction

Background

The propagation of small signals in fluid lines has been of interest to scientists and engineers for many years and, particularly since the advent of fluidic devices in the 1950's. Many investigations have been conducted, both analytical and experimental, in an effort to develop models that can accurately predict the frequency response of fluid-filled transmission lines. Equations, develcped by Nichols (Ref 1) and modified by Krishnaiyer and Lechner (Ref 2), have proven useful in predicting the frequency response under laminar flow conditions.

Brown, Margolis, and Shah (Ref 3) using two and three region viscosity profiles predicted increased attenuation with Reynolds number in lines with fully developed turbulent flow. These models however resulted in relatively complicated solutions. Moore (Ref 4) used a simple constant LRC model as suggested by Brown et. al. (Ref 3) and Funk and Wood (Ref 5) to predict this increased attenuation.

Objectives

The following objectives were established to investigate the effects of turbulent mean flow and oscillatory signals in pneumatic transmission lines .

1. To experimentally determine the small signal response of lines with developed turbulent mean flow.
2. To modify existing computer programs to incorporate new resistance expressions.
3. To develop models for phase shift and attenuation.

II. Theory

Many previous investigations of fluid-transmission lines have successfully used a pneumatic-electrical analogy in their analysis with pressure and volumetric flow rate analogous to voltage and current respectively. Using this analogy the following equations describe the relationship between pressure and volumetric flow:

$$\frac{dP}{dx} = ZQ = (R + j\omega L)Q \qquad (1)$$

and

$$\frac{dQ}{dx} = YP = (G + j\omega C)P \qquad (2)$$

where the complex terms Z and Y are defined as the series impedance and shunt admittance of the line.

Krishnaiyer and Lechner (Ref 2) present Z and Y in round lines with blocked or laminar flow as

$$Z = \frac{8\pi\mu}{A^2}\left[DR\right] + j\left[\frac{\omega\rho}{A} + \frac{8\pi\mu}{A^2}\left[DL\right]\right] \qquad (3)$$

and

$$Y = -\frac{\omega(\gamma-1)\frac{A}{\gamma P}\left[DG\right]}{\left[DC\right]^2 + \left[DG\right]^2} + j\omega\left[\frac{A}{\gamma P} + \frac{(\gamma-1)\frac{A}{\gamma P}\left[DC\right]}{\left[DC\right]^2 + \left[DG\right]^2}\right] \qquad (4)$$

where the terms DR, DL, DG, and DC are given as

$$DR = 3/8 + h_v/4 + 3/(8h_v) \quad (5)$$

$$DL = h_v/4 - 15/(64h_v) \quad (6)$$

$$DG = h_t/2 - 1/(4h_t) \quad (7)$$

$$DC = 1/4 + h_t/2 + 1/(4h_t) \quad (8)$$

with h_v and h_t defined as velocity and temperature distribution parameters given by equations (9) and (10)

$$h_v = 2(\omega/\omega_v)^{1/2} \quad (9)$$

$$h_t = \sigma h_v \quad (10)$$

ω_v is a characteristic frequency defined by Nichols (Ref 1) as

$$\omega_v = \frac{8\pi\nu}{A} \quad (11)$$

These equations are accurate over a frequency range of $0.1\omega_v < \omega < \infty$ for blocked lines and for lines with fully developed laminar flow.

Transmission lines can be described by a propagation operator per unit length Γ and a characteristic impedance Z_o given by equations (12) and (13)

$$\Gamma = (ZY)^{1/2} = \alpha + j\beta \quad (12)$$

$$Z_o = (Z/Y)^{1/2} \quad (13)$$

where α is defined as the attenuation and β is the phase angle per unit length. The input impedance of a line is given as

$$Z_S = Z_O \frac{(Z_T + Z_O)\exp(\Gamma l) + (Z_T - Z_O)\exp(\Gamma l)}{(Z_T + Z_O)\exp(\Gamma l) - (Z_T - Z_O)\exp(\Gamma l)} \qquad (14)$$

The ratio of the recieving pressure to the sending pressure is

$$\frac{P_r}{P_S} = \frac{2Z_T}{(Z_T + Z_O)\exp(\Gamma l) + (Z_T - Z_O)\exp(\Gamma l)} \qquad (15)$$

The gain is the magnitude of the complex pressure ratio given by equation (15)

$$g = \left|\frac{P_r}{P_S}\right| \qquad (16)$$

and in decibels

$$g_{db} = 20 \log_{10} g \qquad (17)$$

The phase shift between the recieving and sending points on the line is the angle formed by the ratio of the imaginary to the real parts of the pressure ratio

$$Beta = \tan^{-1} \frac{Im(P_r/P_S)}{Re(P_r/P_S)} \qquad (18)$$

<u>Turbulent Flow Effects</u>

In order to predict the attenuation for lines with fully developed turbulent mean flow, a constant LRC model is used following the method of Moore (Ref 4). This model uses the turbulent resistance of the line, the adiabatic inertance of the line, and the isothermal capacitance (adiabatic capacitance with $\gamma = 1.0$) of the line to determine the propagation operator and characteristic impedance. The turbulent resistance is defined as

$$R_{vt} = \frac{f Re \mu}{2AD^2} \tag{23}$$

the adiabatic inertance is

$$L_a = \frac{\rho}{A} \tag{24}$$

and the adiabatic capacitance is

$$C_a = \frac{A}{\gamma P} \tag{25}$$

The turbulent impedance is a complex expression consisting of a real term, the turbulent resistance, and an imaginary term, the adiabatic inertance.

$$Z_T = R_{vt} + j\omega L_a \tag{26}$$

Using the adiabatic inertance introduces a small error into the model but greatly simplifies it and reduces computation time. The actual turbulent inertance is slightly greater than the adiabatic inertance, Moore (Ref 4) shows that the turbulent inertance is approximately 3.5% larger than the adiabatic inertance at a Reynolds number of 5,000. The turbulent inertance approaches the adiabatic inertance as the Reynolds number increases.

The turbulent admittance is a complex expression consisting of a conductance (real part) and a capacitance (imaginary part). The capacitance is thought to be isothermal at low frequencies so the expression for the adiabatic capacitance is used (Eq. (25)) with gamma = 1. The conductance is assumed to be zero for the low frequencies at which this model is used

$$Y_t = j\omega C_a \tag{27}$$

Moore (Ref 4) uses the Blasius relation, equation (28), as a simple method of relating fRe to the Reynolds number for turbulent flow.

$$fRe = 0.3164\,Re^{3/4} \tag{28}$$

For laminar flow the expression relating fRe to Reynolds number is Eqn. (29).

$$fRe = 64 \tag{29}$$

The turbulent resistance then becomes

$$R_{vt} = \frac{0.3164\,Re^{3/4}\mu}{2AD^2} \tag{30}$$

and the laminar resistance for this model becomes

$$R_{vl} = \frac{32\mu}{AD^2} \tag{31}$$

The resistance used in this model is a DC resistance, Franke (Ref 6) suggested that using the DC resistance might cause the constant LRC model to predict lower attenuations than would actually be encountered. The constant LRC was modified to account for a possible higher AC resistance. The AC resistance, as suggested by Franke (Ref 6), is

$$R_{vt,AC} = \frac{\rho\mu}{AD}\left\{ f + \frac{\bar{u}}{2}\frac{\partial f}{\partial \bar{u}} \right\} \tag{32}$$

After carrying out the differentiation and simplifying the expression, the AC resistance becomes

$$R_{vt,AC} = 1.75\, R_{vt} \tag{33}$$

while the expression for the laminar resistance will not change.

The attenuation predicted by the constant LRC model, using both the DC and AC resistance, is nondimensionalized using the method of Brown (Ref 3) and plotted against a nondimensional freque⁻ Ω in Fig 1. The attenuation predicted by Nichols equations, as approximated by Krishnaiyer and Lechner (Ref 2), is also shown as a reference. Fig. 1 shows that the constant LRC models predict attenuations higher than those predicted by Nichols below

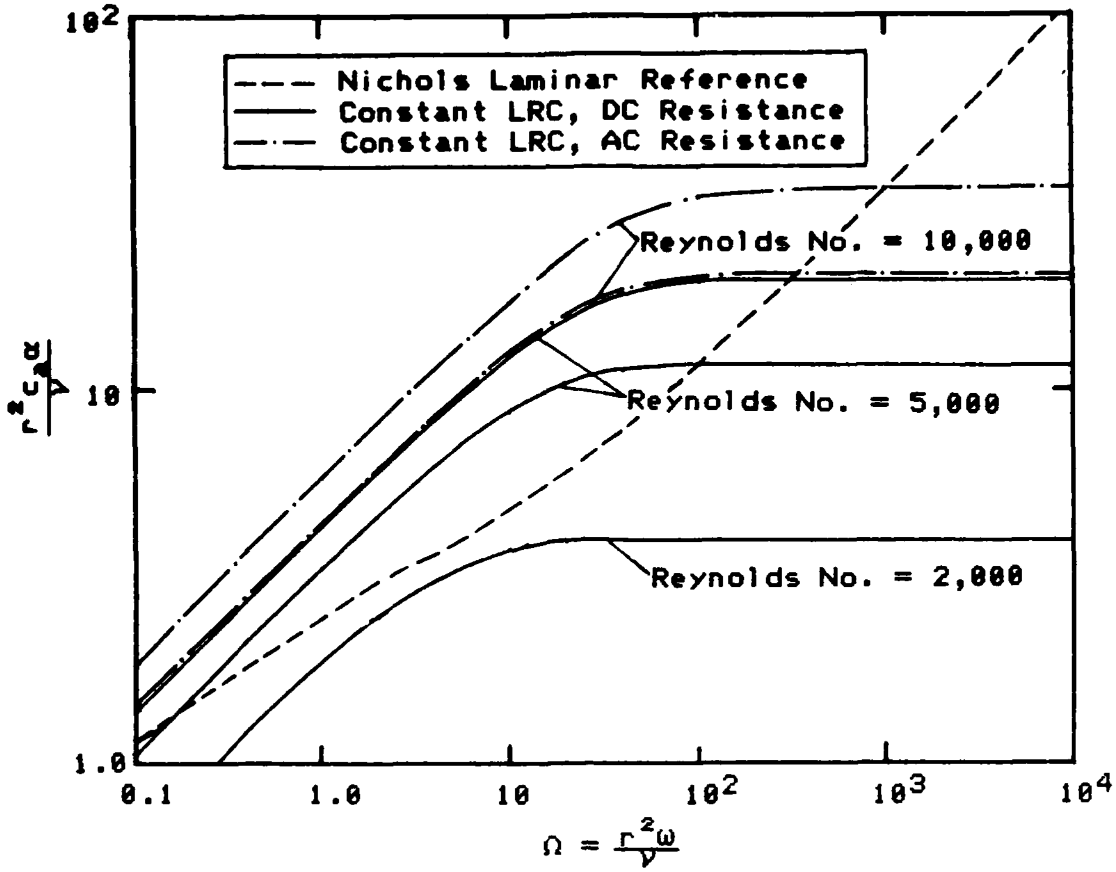

Figure 1 Predicted Attenuation vs Frequency

certain frequencies, but reach constant attenuations that result in under prediction at higer frequencies. The frequency at which the turbulent and laminar curves intersect is denoted as the break frequency Ω_b. The dimensional break frequency ω_b is obtained from Ω_t. The actual behaviour of lines with turbulent flow has been experimentally proven by Brown, et. al. (Ref 3) and Funk and Wood (Ref 5) to be laminar at frequencies higher than the break frequency. The behaviour in the vicinity of the break frequency is uncertain, experiments by Margolis and Brown

(Ref 7) produced large deviations in attenuation in the vicinity of the break frequency.

The computer program used in this study employed the turbulent constant LRC model at frequencies below the break frequency, ω_b ,and the laminar model (Eqns. (3) and (4)) at frequencies greater than the break frequency. The program uses these models to determine the propagation operator and characteristic impedance (Eqns. (12) and (13)) then uses Eqns. (14) and (15) to determine the theoretical pressure ratio. The program then uses Eqns. (16), (17), and (18) to compute the theoretical gain and phase shift.

Mean Pressure Drop

Schlichting expresses the relation between pressure drop and distance in a constant area duct as

$$\Delta \bar{P} = -f \frac{l}{D} \frac{\rho \mu^2}{2} \qquad (34)$$

If equation (28) is used to determine f and substituted into equation (34) then the pressure drop can be expressed as a function of velocity and Reynolds number. Further manipulation with the velocity and density can result in equations (35) and (36) which express the pressure drop as a function of l, D, Re, ρ, and μ for turbulent and laminar flows respectively.

$$\Delta \bar{P} = -0.1582 \frac{l}{D} \frac{\mu^2}{\rho D^2} Re^{1.75} \qquad (35)$$

$$\Delta\bar{P} = -32\frac{l}{D}\frac{\mu^2}{\rho D^2}Re \tag{36}$$

Equations (35) and (36) are only applicable for incompressible flow. To find the pressure drop in small diameter lines at high Reynolds numbers, Eqns. (35) and (36) are rewritten as infinitesmal pressure drops for a small distance dx. The ideal gas law is used to express density in terms of pressure and temperature, then assuming that Reynolds number and temperature are constant in the line the equations can be integrated to get Eqns. (37) and (38).

$$\Delta\bar{P} = \bar{P}_e - \left[0.15[illegible]\,\frac{l\mu^2}{D^3}R_g T\,[illegible]^{1.75} + \bar{P}_e^2\right]^{1/2} \tag{37}$$

$$\Delta\bar{P} = \bar{P}_e - \left[[illegible]\right]^{1/2} \tag{38}$$

III. Experimental Apparatus

The experimental apparatus consisted of pneumatic signal generating equipment and signal analysis instrumentation shown schematically in Fig. 2. A rotometer was also used to verify that the mean flow was consistent with the pressure drop.

The wave analyzer connected to the sending dynamic pressure transducer was used to generate a sinusoidal signal. This signal was then amplified and sent to the pneumatic signal generating equipment which amplified it further and sent it to the pneumatic signal generator. A frequency counter was used to accurately determine the actual frequency of the signal generated by the wave analyzer.

The signals in the line were measured by two dynamic pressure transducers. These signals were sent to charge amplifiers. The amplified signal was then passed to the dual beam oscilloscope and to the two wave analyzers. The oscilloscope was used to monitor the signal and to measure the phase delay. The wave analyzers were used to measure the RMS output voltage of the signals.

The mean flow rate was established using the rotometer. Once the mean flow rate was established the rotometer was removed and the flow rate was monitored using the static pressure transducer. The losses associated with the rotometer were small enough that its removal caused

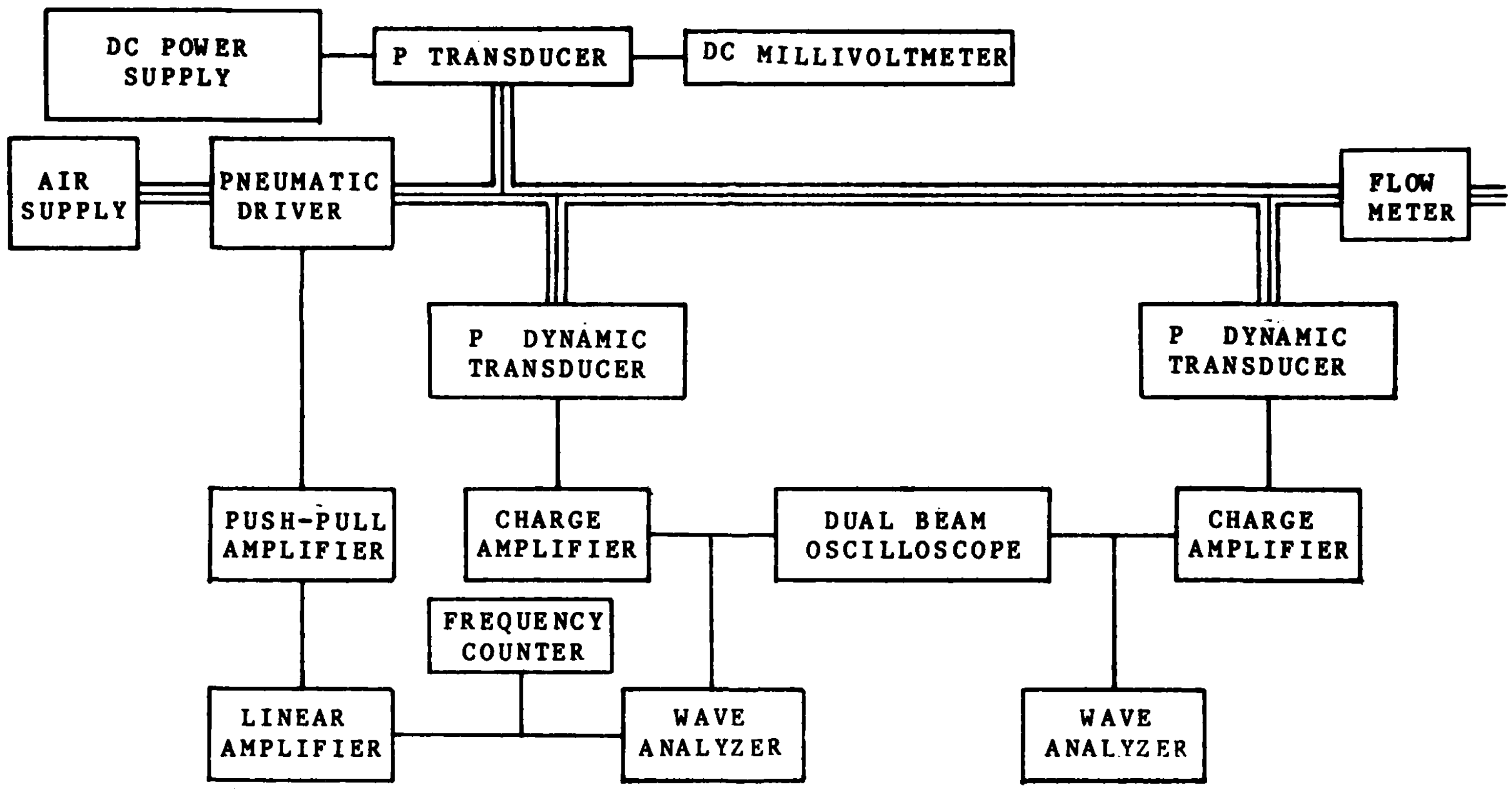

Figure 2 Schematic Diagram of Experimental Apparatus

negligible changes in flow rate. The rotometer was calibrated before any tests were conducted.

Test Configurations

Six different line configurations were used for the experiment. A schematic of the basic line configurations is shown in Fig 3. Each test line consisted of plexiglas fixtures at each end which contained the transducer cavities and a smooth steel line of constant diameter between the two plexiglas blocks. The lines were smooth enough to accurately predict the pressure drop in the line using equation (37) for turbulent flow and equation (38) for laminar flow.

Classification of Cases

The cases were designated using a two digit system. The first digit indicates the line being tested and corresponds to the line numbers used in Table I. The second digit refers to the Reynolds number at which the line is being tested. A one indicates a Reynolds number of 2000, a two indicates a Reynolds number of 5000, and a 3 indicates a Reynolds number of 10000. For example case 52 is line 5 tested at a Reynolds number of 5000.

Line 1 was tested in several different configurations before taking data for all of the lines at the various Reynolds numbers. One test was to verify that the length of the line from the pneumatic signal generator to the test lines did not have an adverse effect on the signals and the

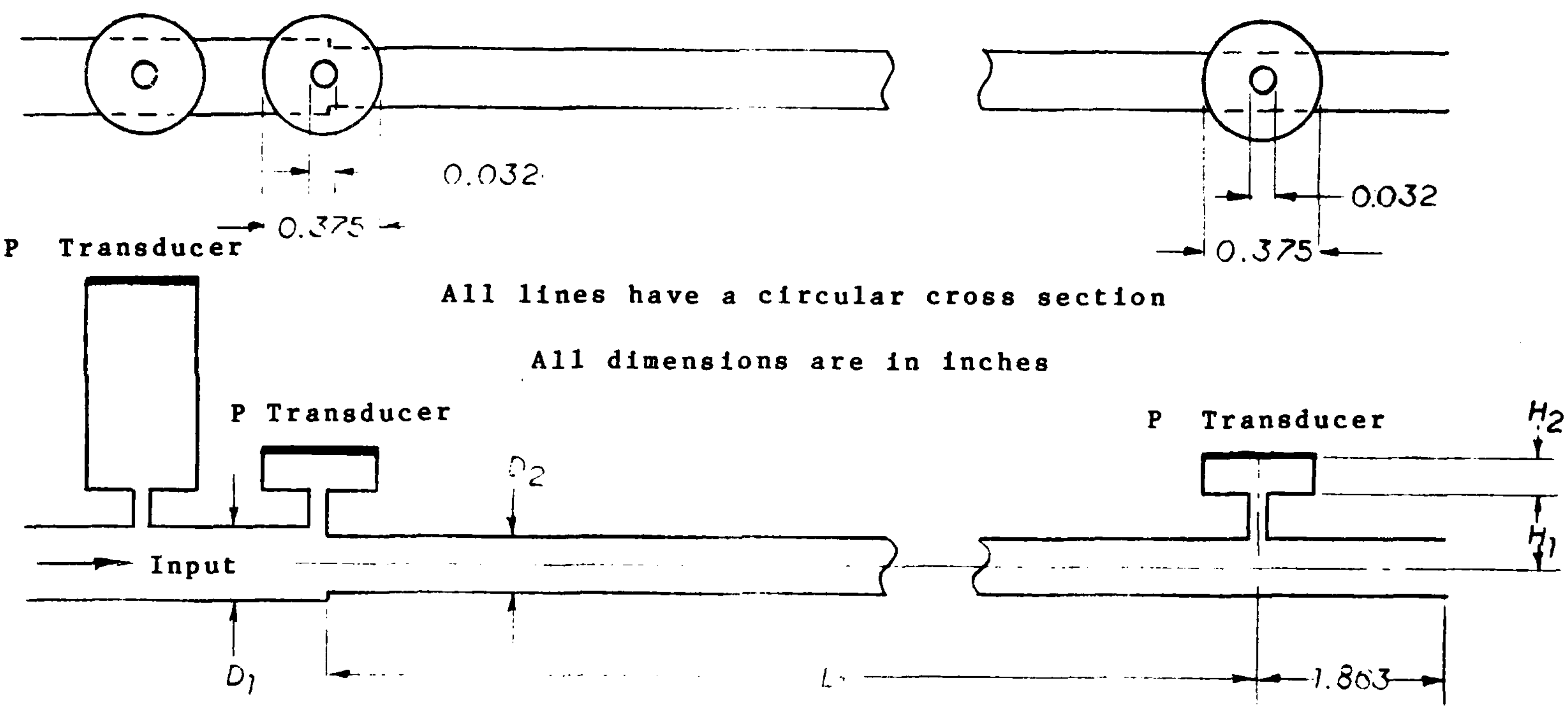

For values of D_1, L , , and L_1 see Table I

Figure 3 Test Line Configuration

Table I

Line dimensions for different configurations

Line number	D	D	H	H	L
1	0.251	0.195	0.181	0.029	24.00
2	0.190	0.119	0.190	0.029	24.00
3	0.065	0.041	0.202	0.029	24.00
4	0.251	0.195	0.186	0.028	36.00
5	0.190	0.119	0.182	0.026	36.00
6	0.065	0.041	0.187	0.027	36.00

All dimensions are in inches

other to determine the effect of the volume immediately beneath the dynamic transducers. These two cases were tested at Reynolds number 2000 on line 1 and were designated cases 11A and 11B respectively.

IV. Experimental Procedure

The same procedure was used consistently to collect data for each test. Equation (37) or (38) was used to calculate a pressure drop for the line at the Reynolds number desired. The output of the static pressure transducer was then used to set up the equivalent pressure drop. The rotometer was then used to verify that the flow rate was correct for the case. The rotometer was then removed and the static transducer was used to monitor the mean pressure for any variations in flow rate. Test runs were made at Reynolds numbers of 2000, 5000, and 10000 for the four smaller diameter lines. The two 0.195 diameter lines were run at Reynolds numbers of 2000 and 5000 due to the mass flow constraints of the pneumatic signal generator.

The barometric pressure and temperature in the room were recorded before each test run. The desired flow rate was set using the procedure outlined above then the wave analyzer was used to set the frequency of the signal. The RMS output of the sending and recieving transducers was recorded from the wave analyzers and the phase lag was measured on the oscilloscope.

V. Results and Discussion

The computer program used to predict the theoretical gain and phase shift was based on that used by Malanowski (Ref 9). It was extensively modified to incorporate the constant LRC turbulent models. In order to verify that the original laminar section still functioned, the program was used to predict the gain and phase shift in a blocked line. Then, the program was used to predict the gain and phase shift for each of the six lines with laminar mean flow. Table II gives a summary of test conditions and some experimental and theoretical data for the cases with Reynolds numbers of 2000. Figures 4-18 show the experimental and theoretical gains and phase shifts for these cases.

There are no phase diagrams for line 6 at any of the Reynolds numbers tested; this is due to the fact that the noise in line 6 made accurate collection of phase lag impossible. This is also true of several of the other lines at higher Reynolds numbers.

Figures 4-18 verify that Nichols equations are very good at predicting both the gain and phase shift for lines with laminar mean flow. Only cases 31 and 61 show major discrepancies, occuring mainly at lower frequencies. This may be partially due to noise problems, described above, which were associated with the two smallest lines. All of the laminar curves however, showed a 1-2 db error at

Table II

Test conditions

Case Number	$\bar{P}$ psig	Q cis	Re	$\bar{u}$ fps	ω_v rad/sec	P_a psia	T_a deg F
11	0.016	7.61	2012	21.2	20.8	14.37	75.2
11A	0.016	7.61	2012	21.2	20.8	14.37	75.2
11B	0.016	7.61	2012	21.2	20.8	14.37	75.2
12	0.116	18.93	5003	52.8	20.8	14.30	75.2
21	0.069	4.58	1992	34.3	55.7	14.39	75.2
22	0.493	11.18	4944	83.8	54.8	14.39	75.2
23	1.554	21.29	9695	159.5	53.2	14.39	77.0
31	1.616	1.50	2012	94.7	448.5	14.53	77.0
32	9.657	3.03	5037	191.3	361.5	14.45	77.9
33	23.385	4.42	9814	279.0	270.7	14.40	80.6
41	0.023	7.69	2042	21.5	20.7	14.39	75.2
42	0.164	18.66	4974	52.1	20.6	14.39	75.2
51	0.099	4.58	1986	34.3	55.9	14.34	77.0
52	0.697	11.05	4974	82.8	54.1	14.52	76.1
53	2.233	21.06	9884	157.8	51.6	14.52	77.0
61	2.276	1.48	1996	93.4	446.6	14.37	78.8
62	9.514	2.46	4059	155.3	363.5	14.39	78.8
63	21.289	3.48	7457	219.7	280.3	14.39	78.8

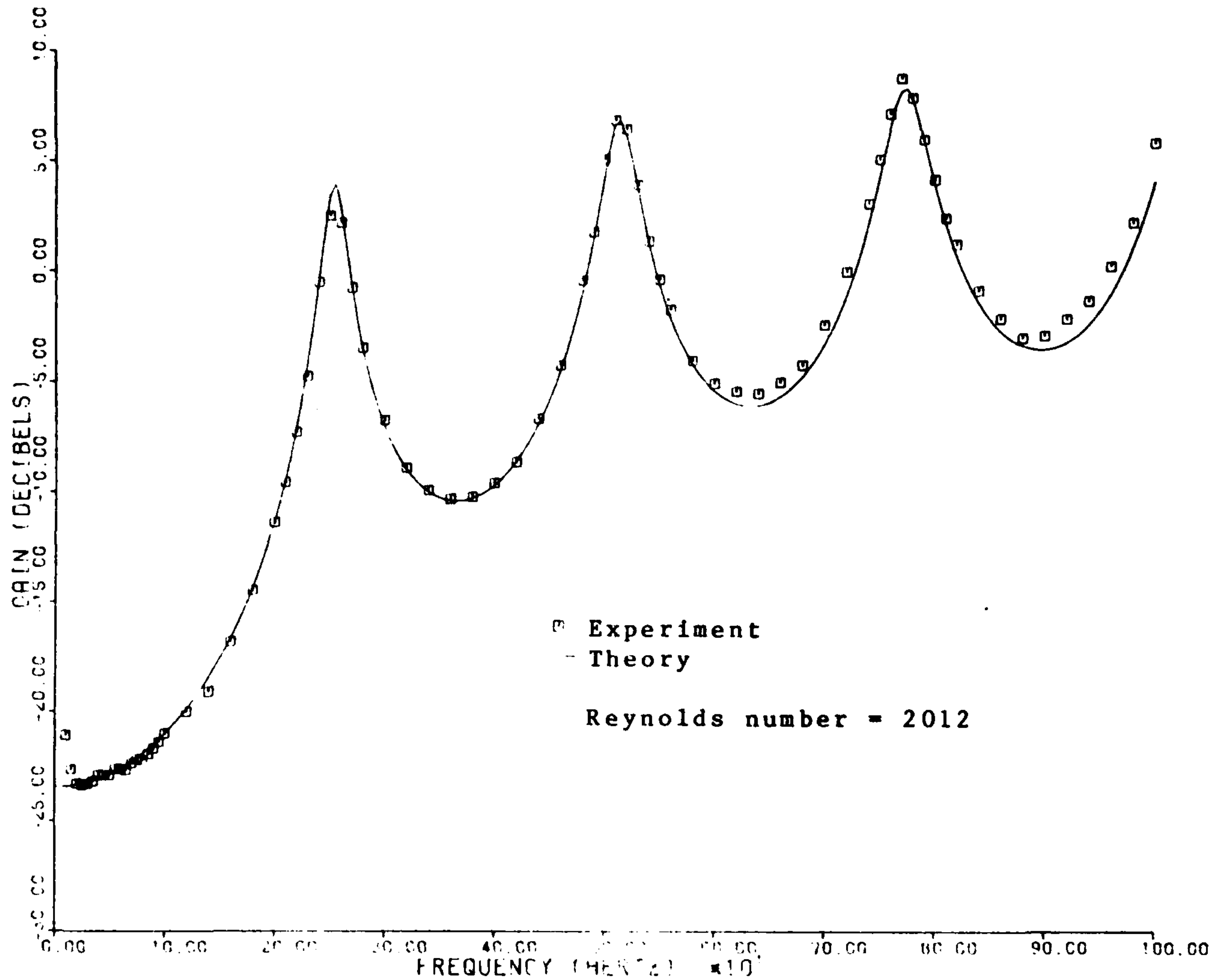

Figure 4 Experimental and Theoretical Gain vs Frequency for Case 11

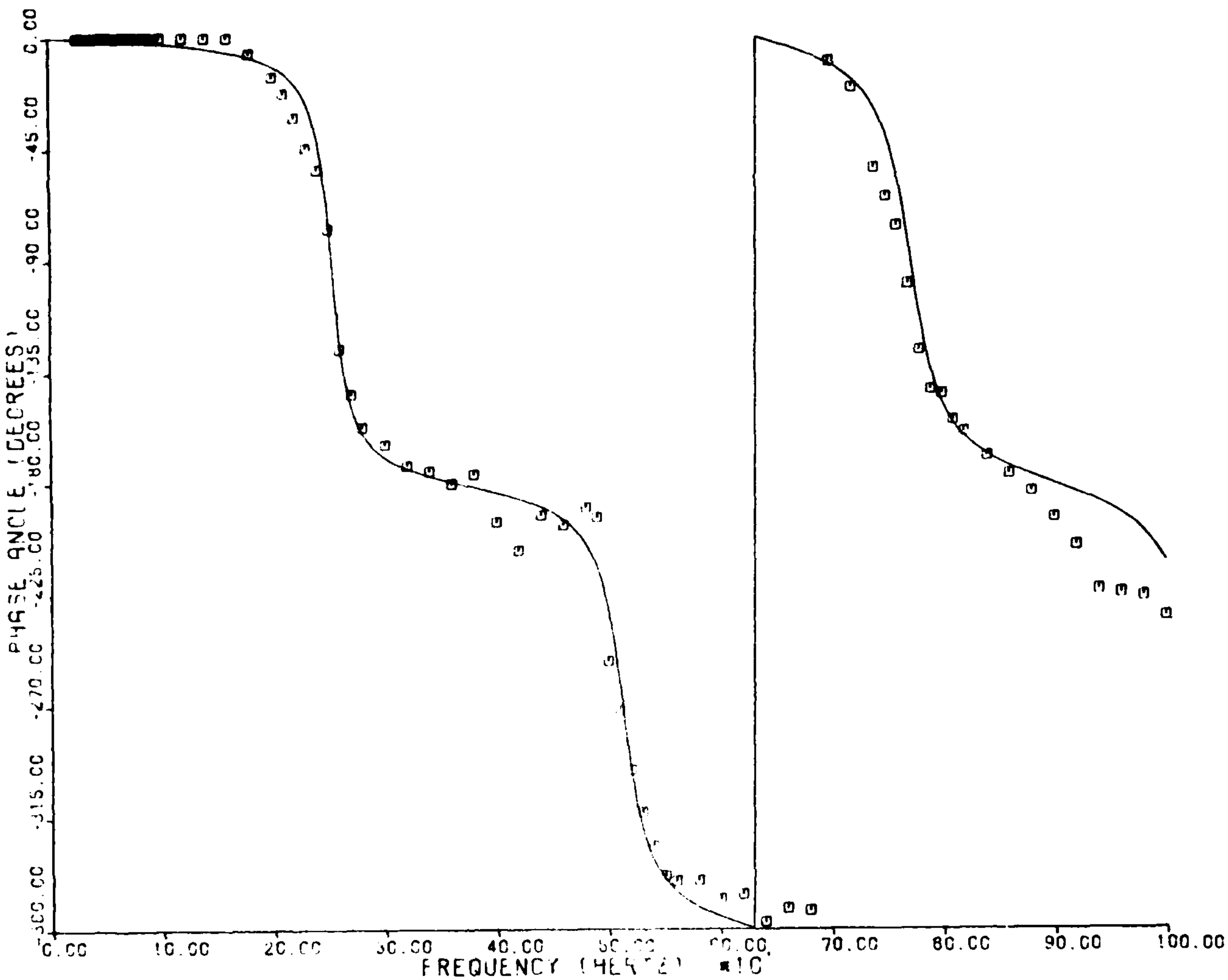

Figure [illegible] Experimental and Theoretical Phase vs Frequency for Case 11A

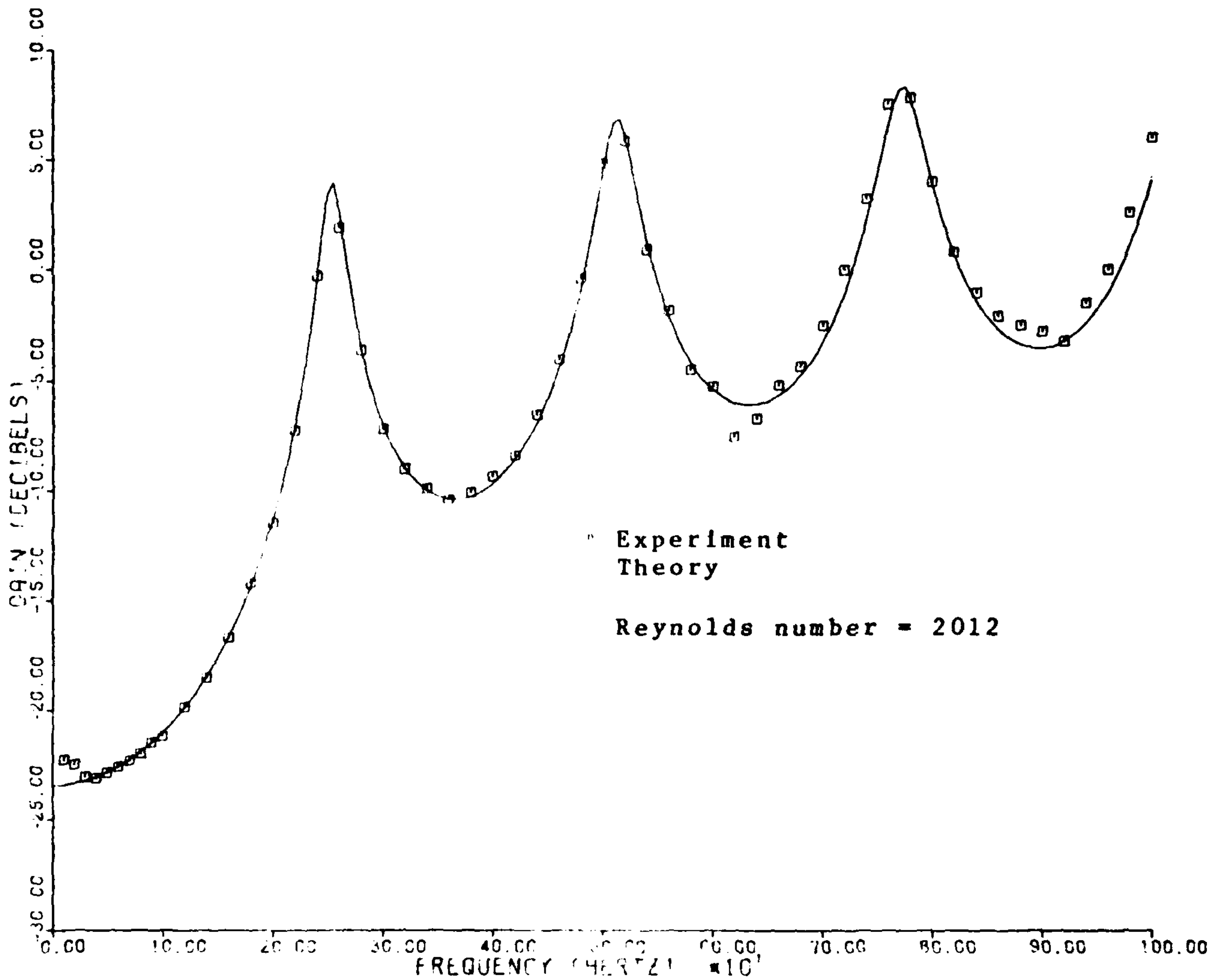

Figure 6 Experimental and Theoretical Gain vs Frequency for Case 11A

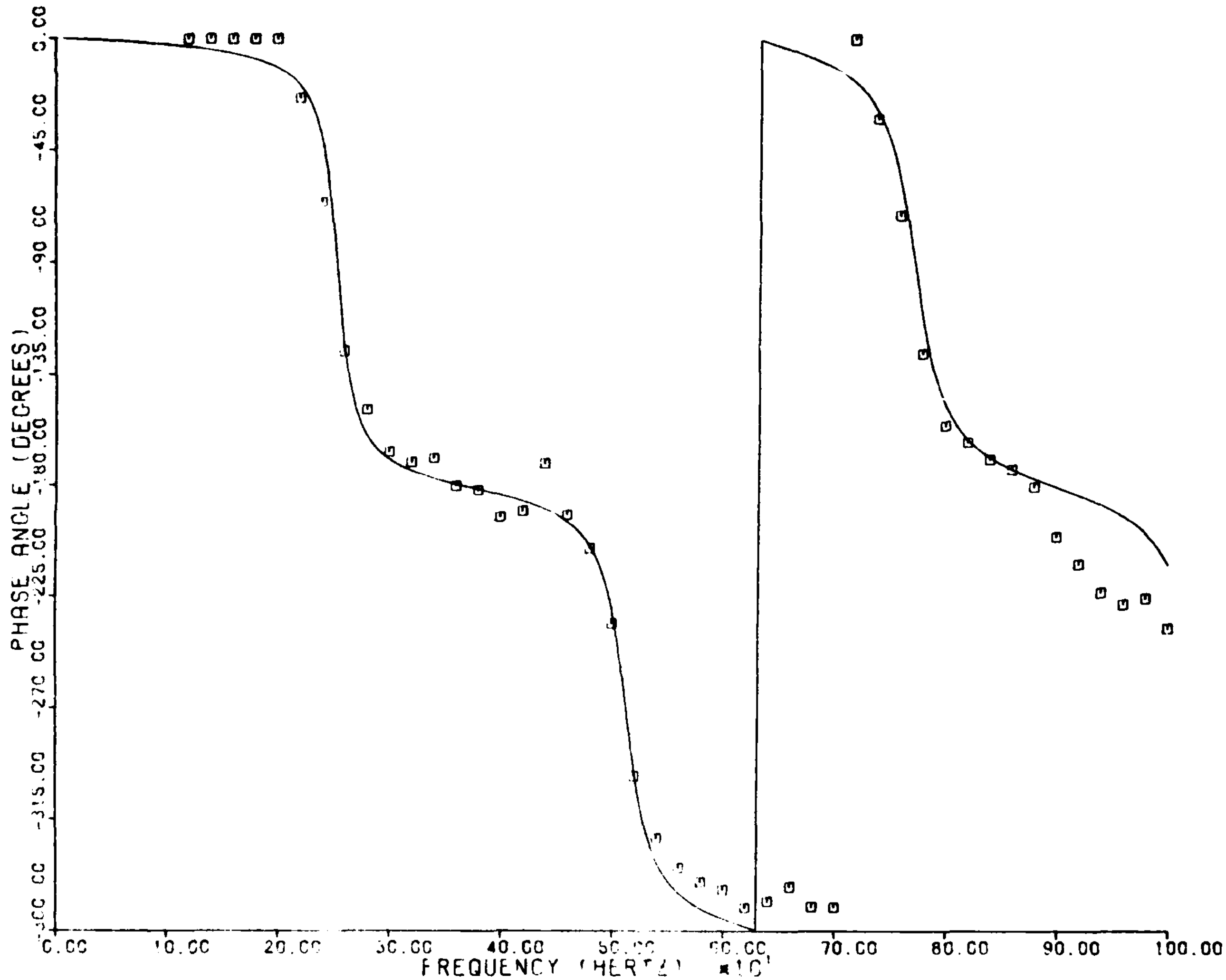

Figure 7 Experimental and Theoretical Phase vs Frequency for Case 11A

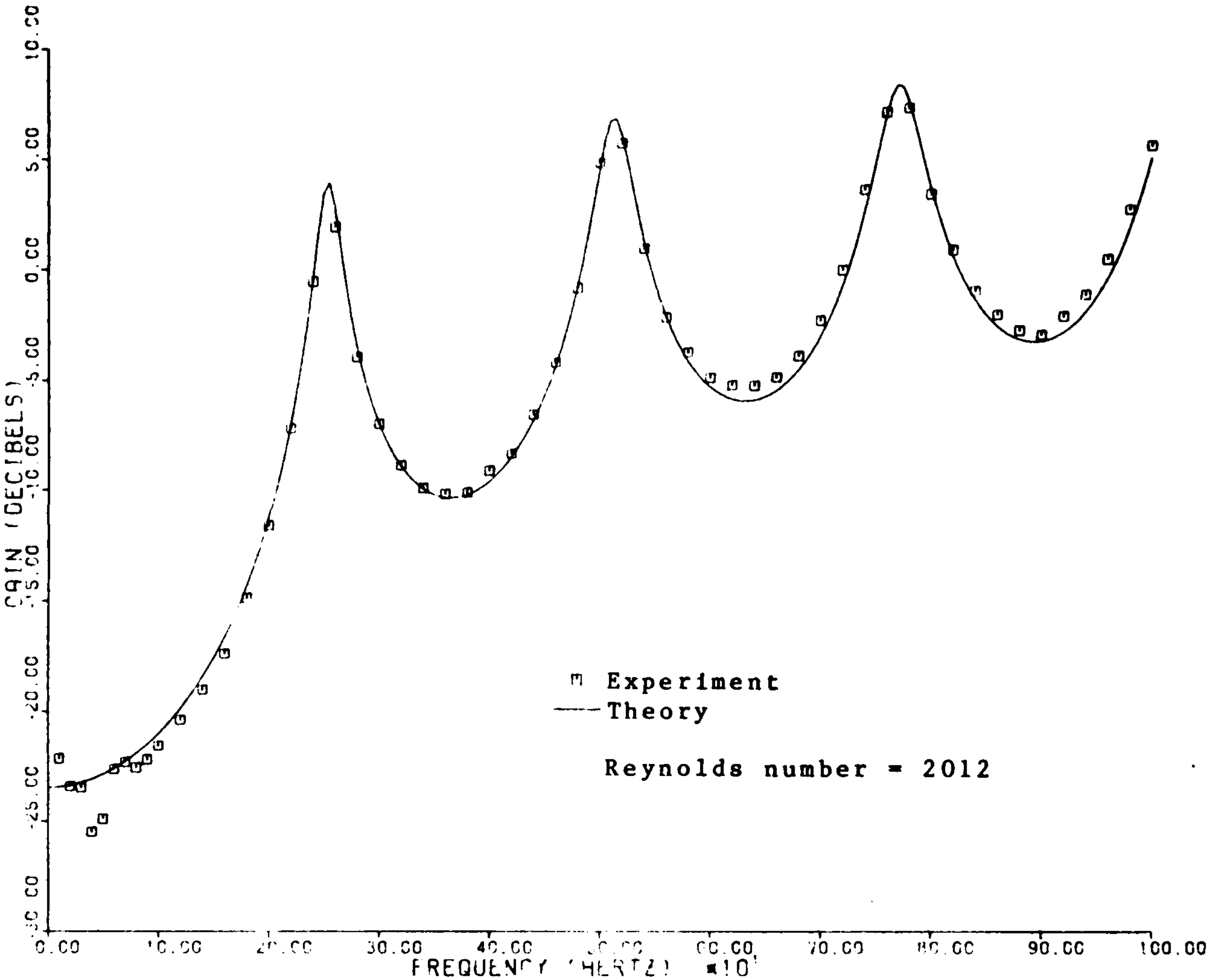

Figure 8 Experimental and Theoretical Gain vs Frequency for Case 11B

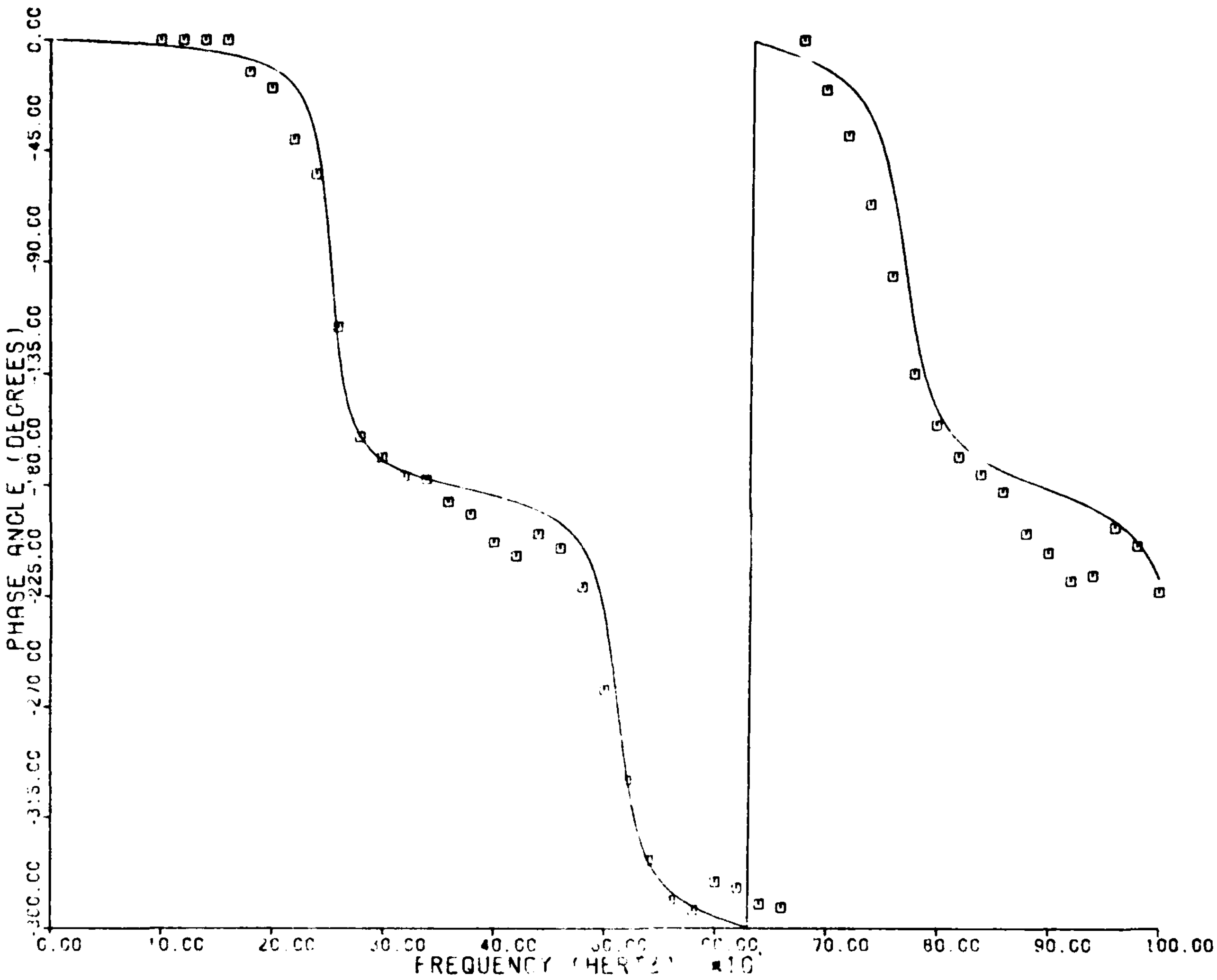

Figure 9 Experimental and Theoretical Phase vs Frequency for Case 11B

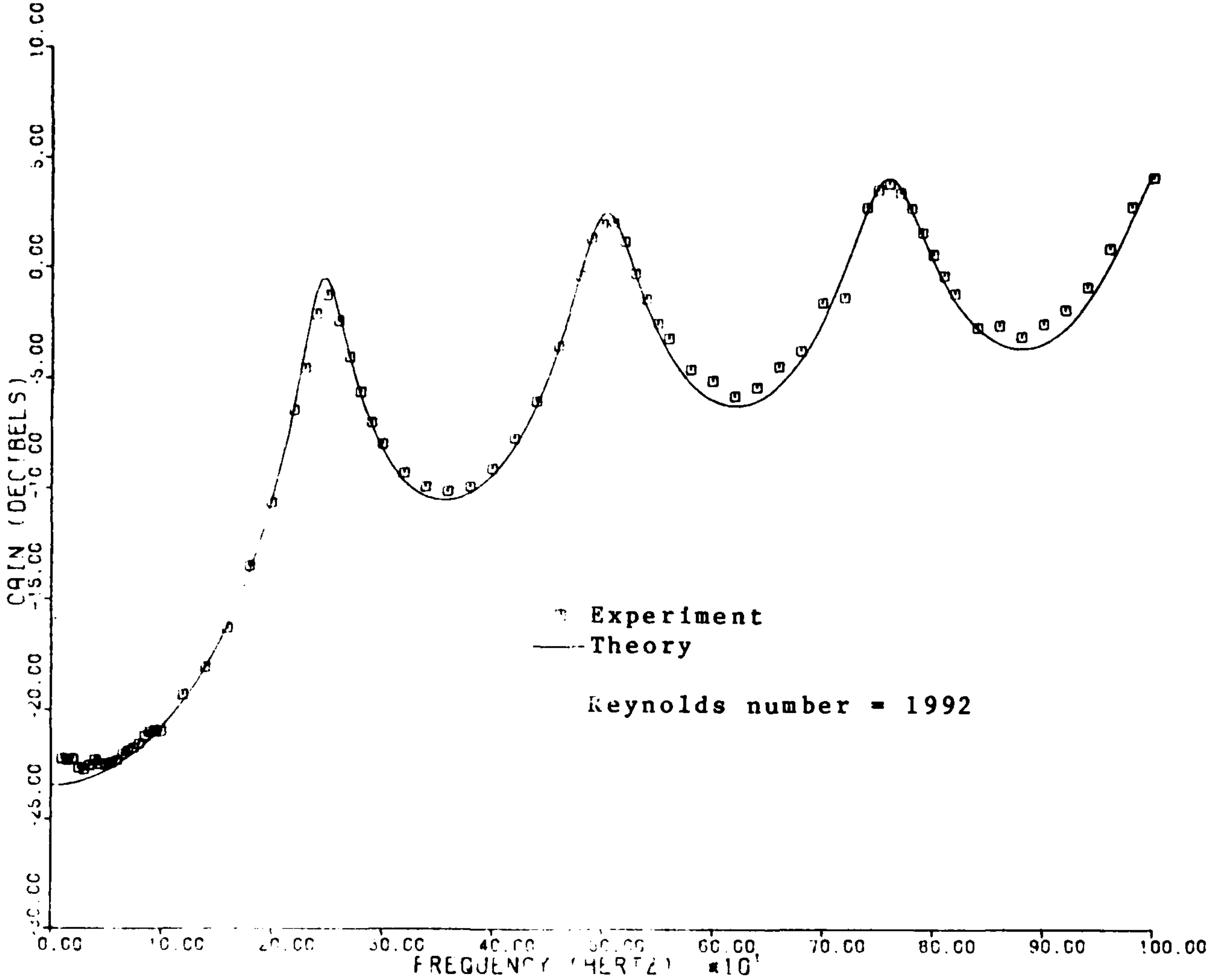

Figure 10 Experimental and Theoretical Gain vs Frequency for Case 21

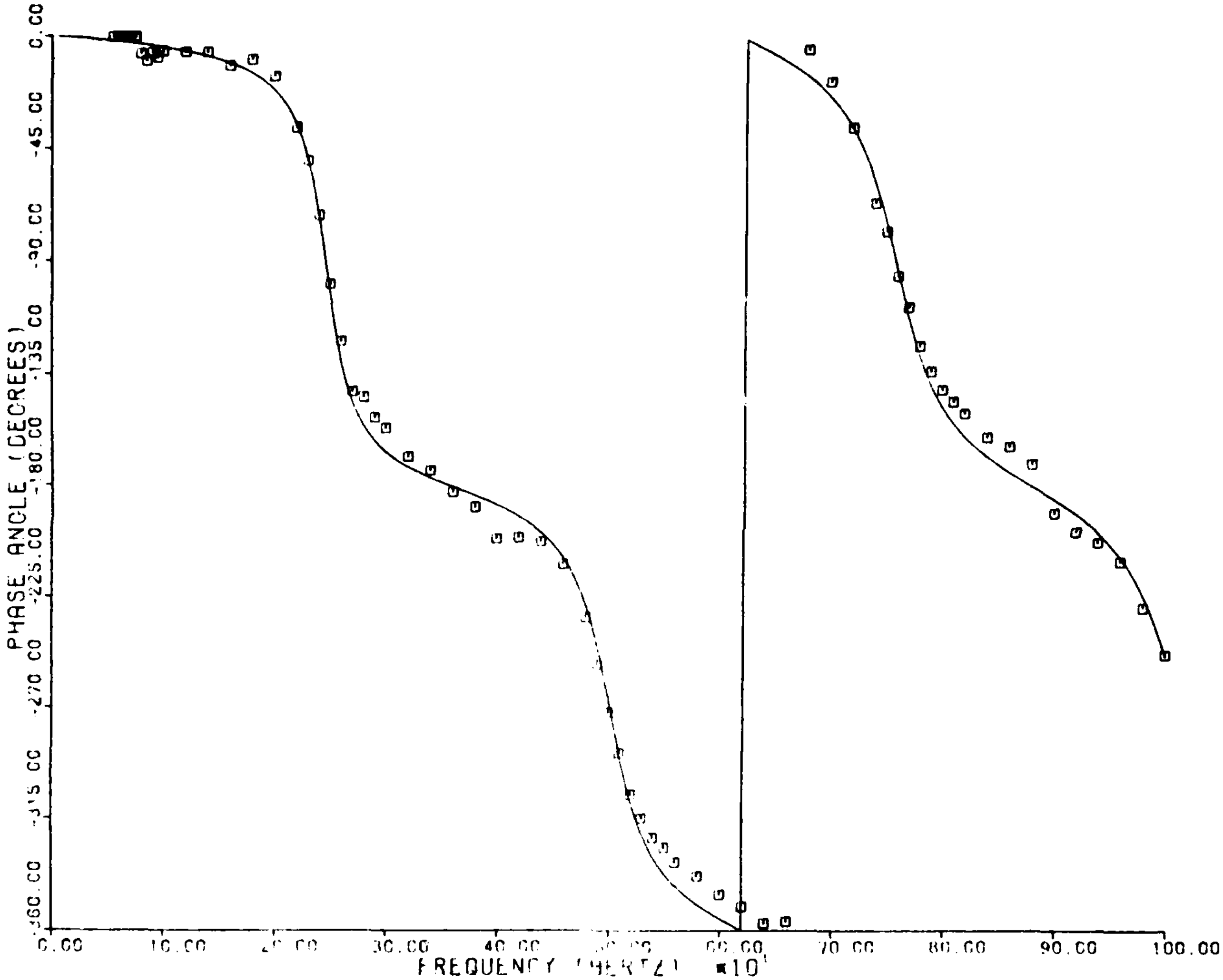

Figure 11 Experimental and Theoretical Phase vs Frequency for Case 21

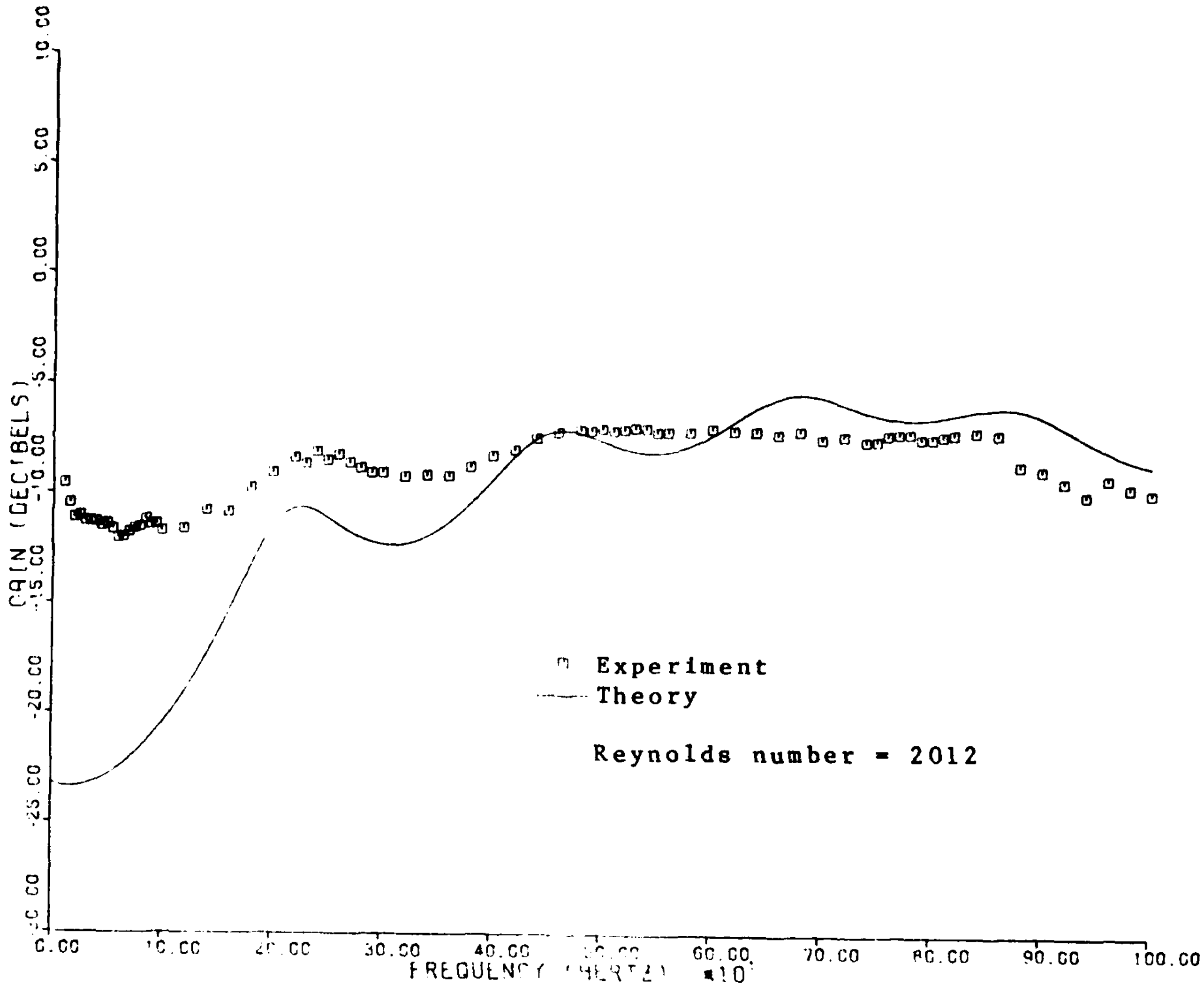

Figure 12 Experimental and Theoretical Gain vs Frequency for Case 31

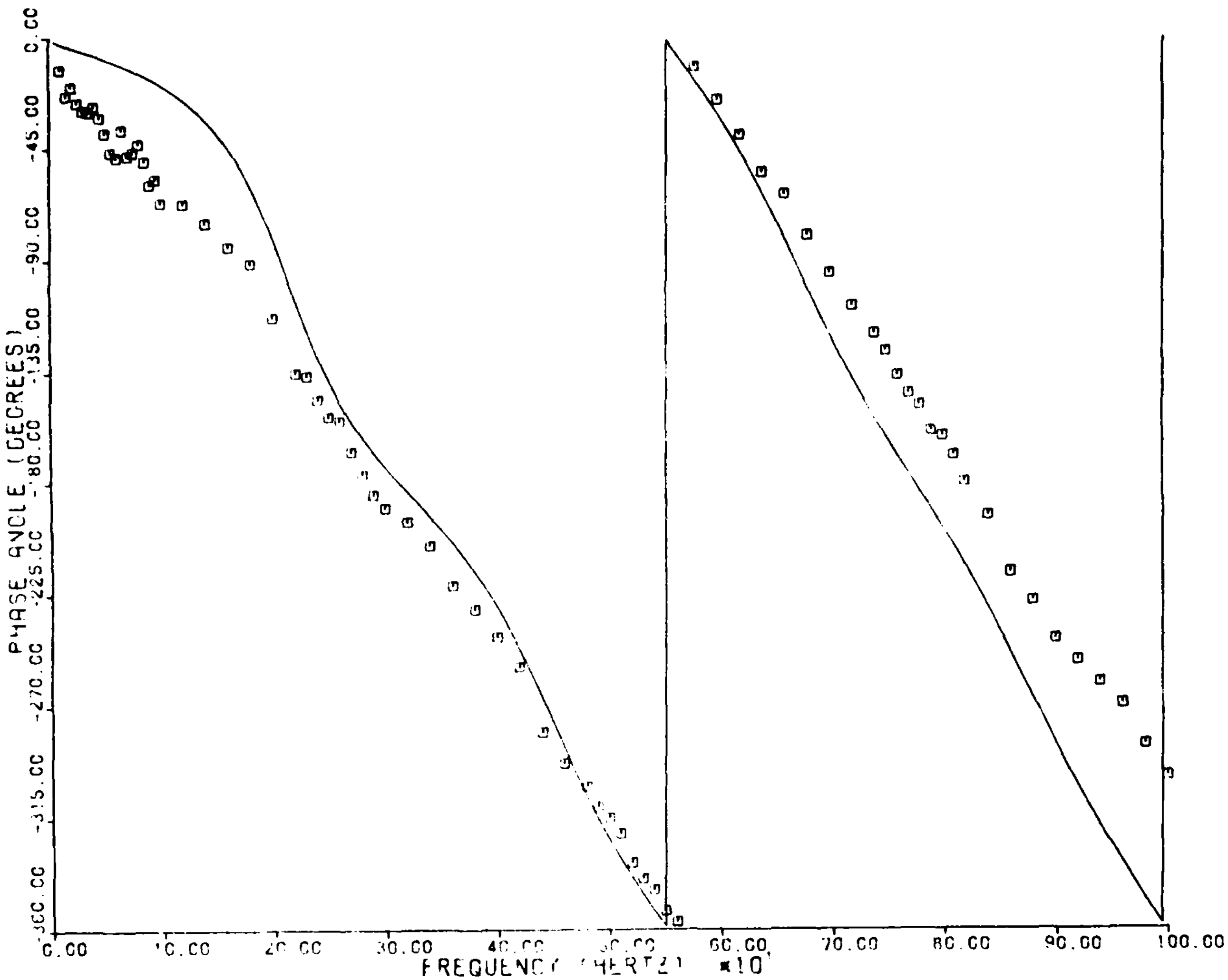

Figure 13 Experimental and Theoretical Phase vs Frequency for Case 31

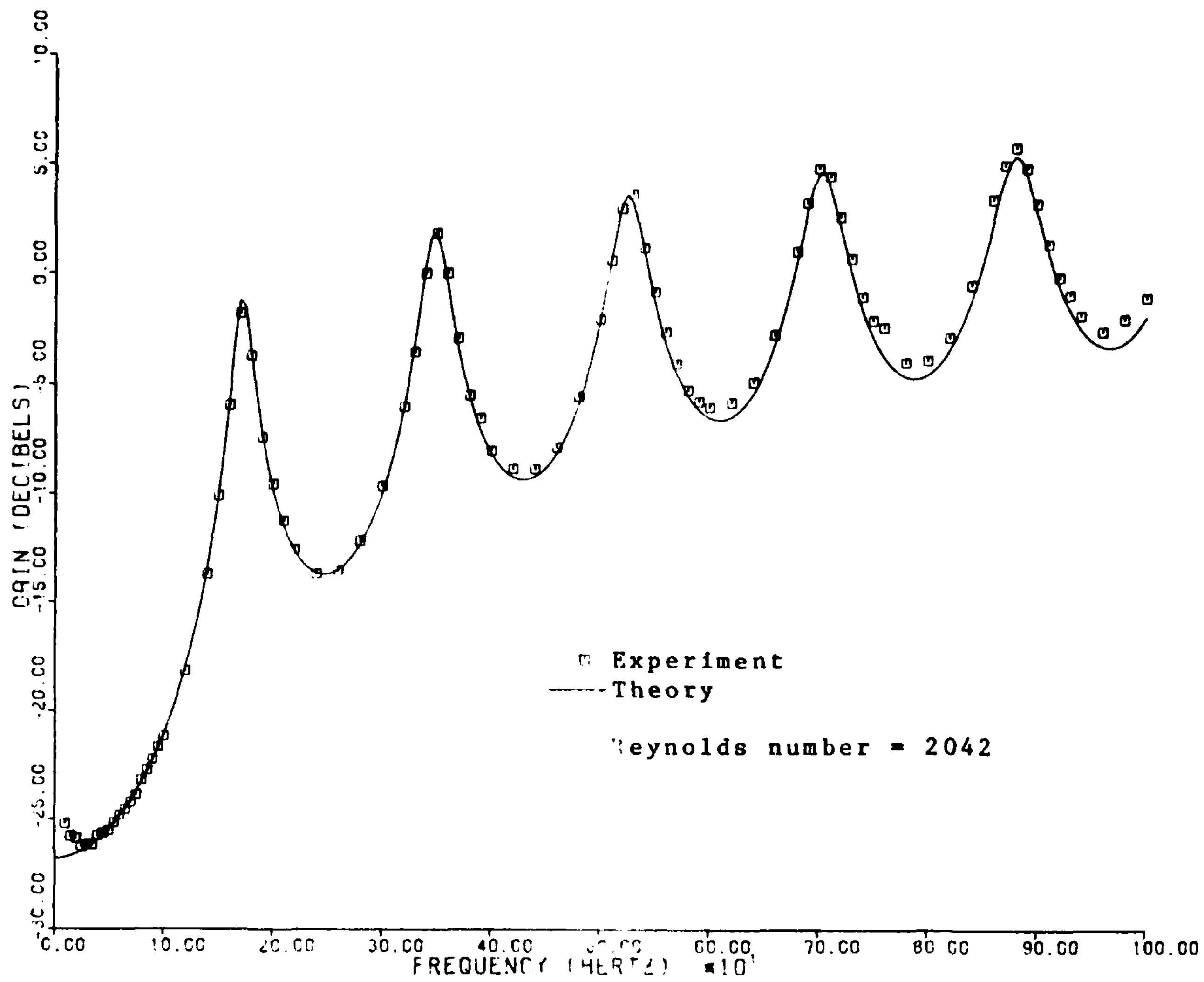

Figure 14 Experimental and Theoretical Gain vs Frequency for Case 41

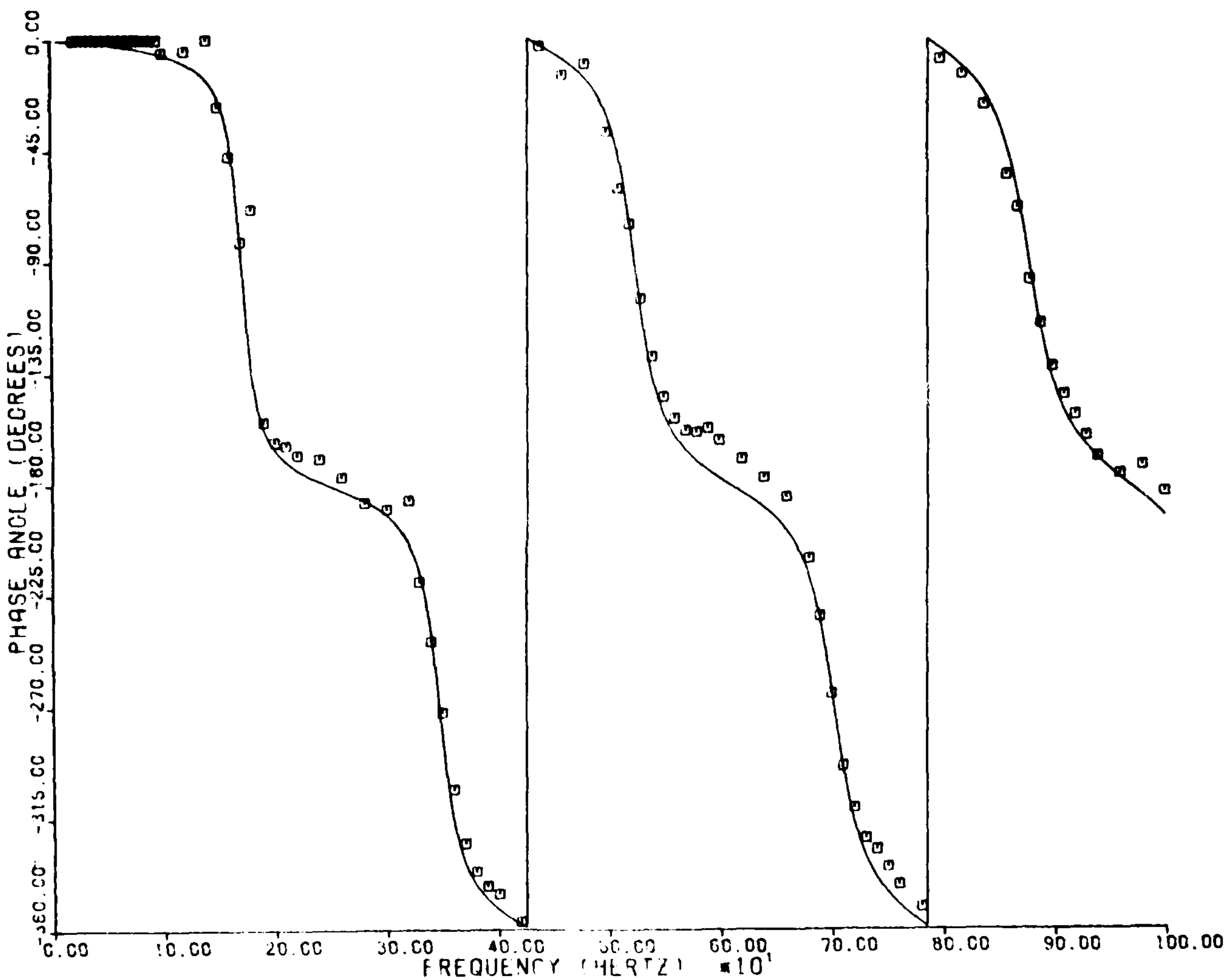

Figure 15 Experimental and Theoretical Phase vs Frequency for Case 41

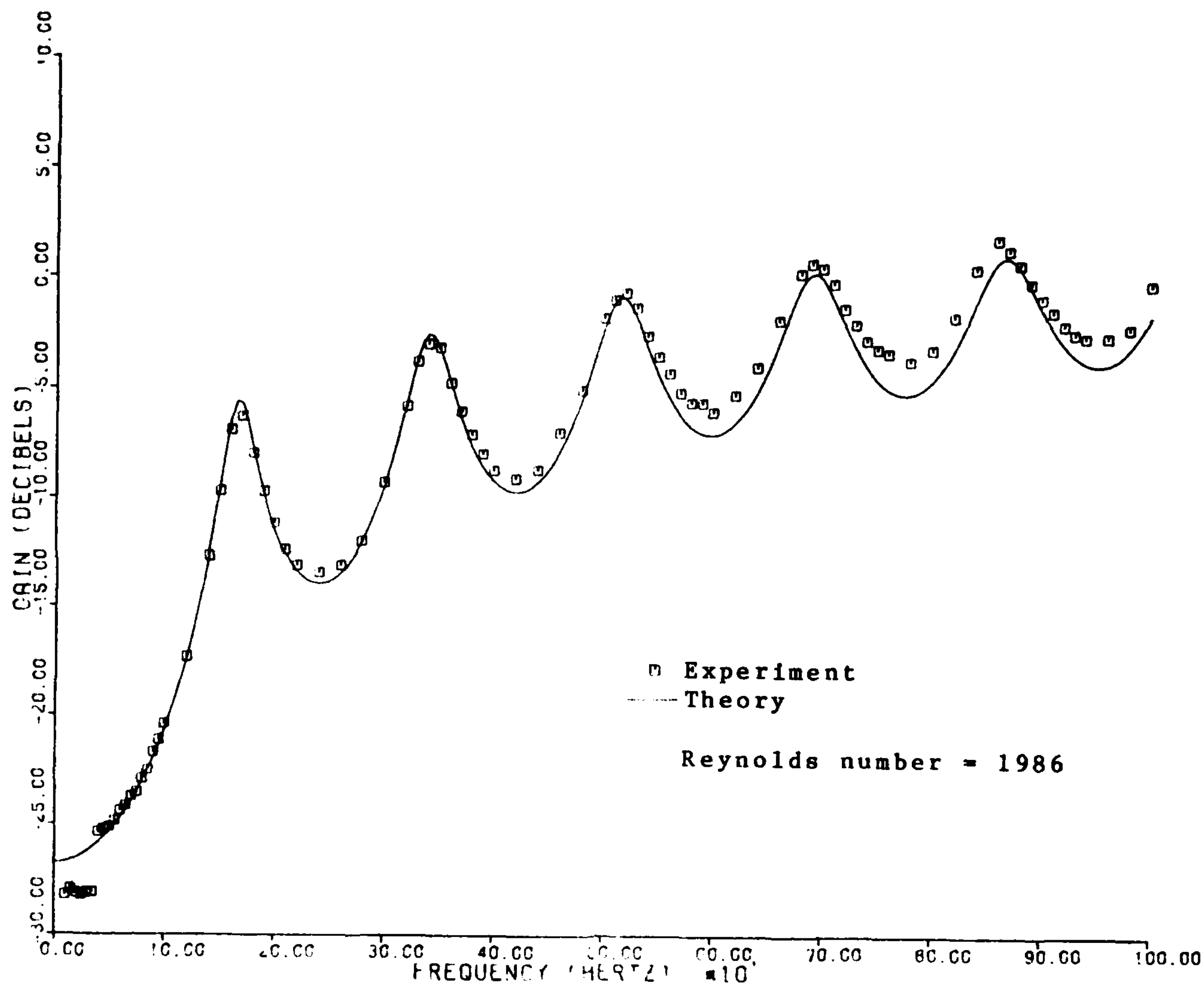

Figure 16 Experimental and Theoretical Gain vs Frequency for Case 51

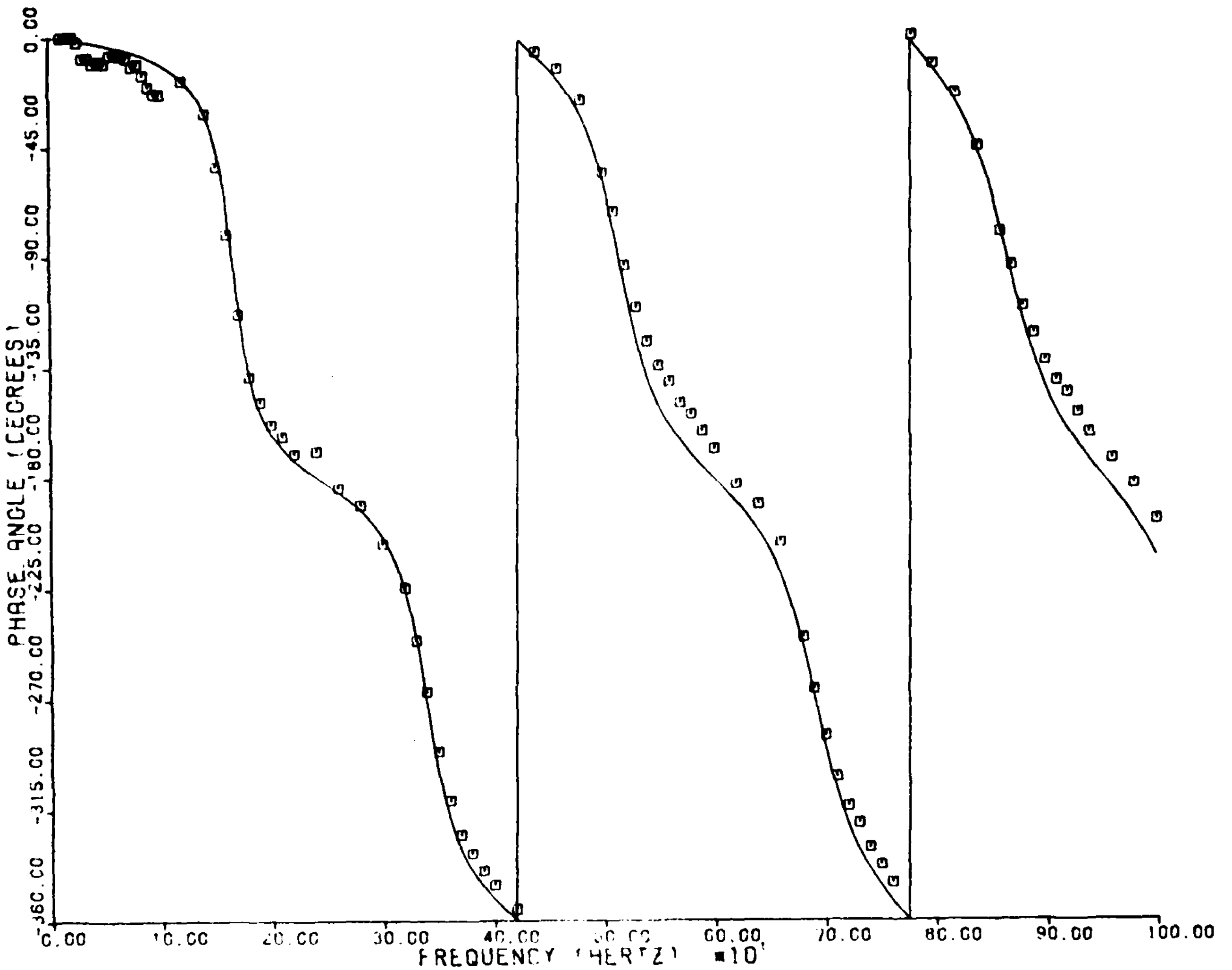

Figure 17 Experimental and Theoretical Phase vs Frequency for Case 51

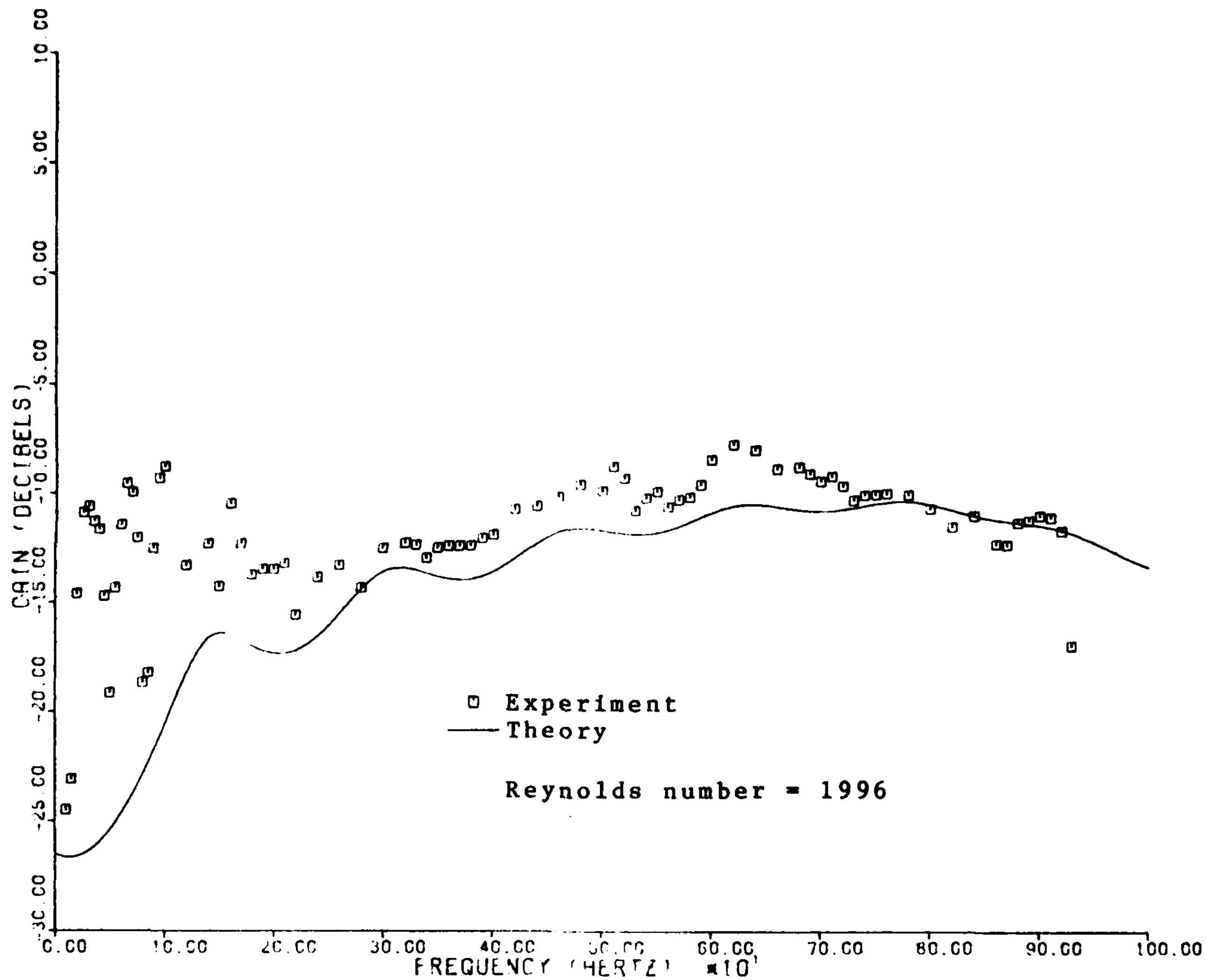

Figure 18 Experimental and Theoretical Gain vs Frequency for Case 61

frequencies below approximately which approaches the low frequency limit for which Krishnaiyer and Lechners equations are applicable.

Turbulent Flow

Figures 19-34 show the gain and phase shift for Reynolds numbers from 5,000 to 10,000. Table III gives the value of the nondimensional frequency (used in Fig. 1) which corresponds to the highest tested frequency of 1000 hz for each case. The value of , which corresponds to the intersection of the laminar and turbulent attenuation curves is also found in Table III for both AC and DC resistance.

The method used to predict the gain and phase shift employed the turbulent model up to the break frequency . From this frequency up Krishnaiyer and Lechners equations were used to predict the gain and phase shift. Because of this the curves representing the constant LRC models are only plotted up to their break frequency.

Figures 19-26 show the theoretical gain and phase shift and the experimental gain and phase shift for four of the lines at a Reynolds number of 5,000. The figures show that Nichols theory is accurate above the break frequency. Figures 27-28 show large discrepancies in all of the theories although the constant LRC with AC resistance is good at high frequencies. The constant LRC models appear to be inadequate to predict the phase shift for any Reynolds number tested while Krishnaiyer and Lechners equations

Table III

Values of Ω_{max}, $\omega_{b,DC}$, and $\omega_{b,AC}$ for the Turbulent cases

Case Number	Ω_{max} 1000 Hz	$\omega_{b,DC}$ rad/sec	$\omega_{b,AC}$ rad/sec
12	2416	260	878
22	919	684	2311
23	946	2005	6639
32	141	4450	15040
33	188	10061	33313
42	2437	257	871
52	931	675	2282
53	976	1945	6441
62	140	4473	15120
63	182	10420	34503

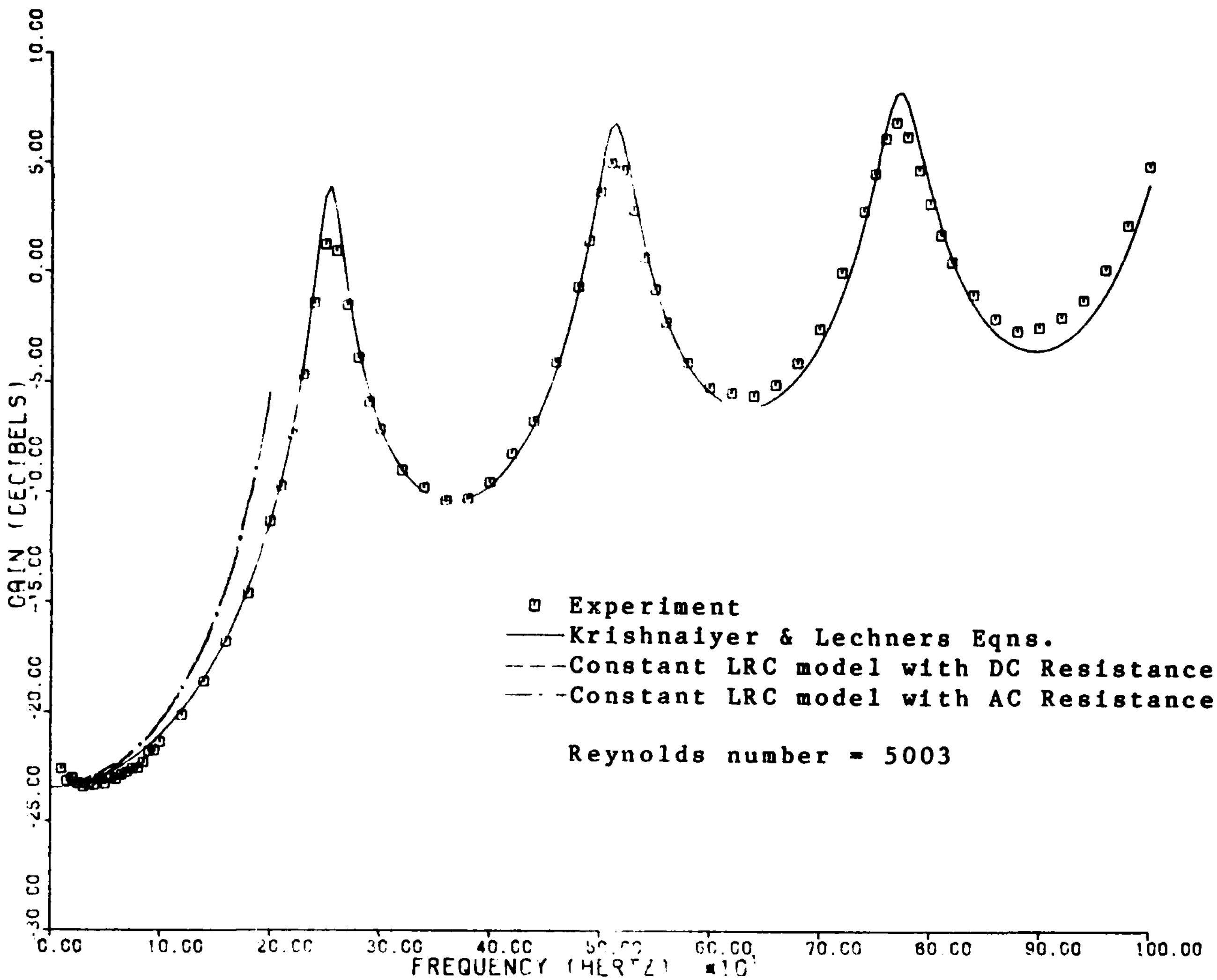

Figure 19 Experimental and Theoretical Gain vs Frequency for Case 12

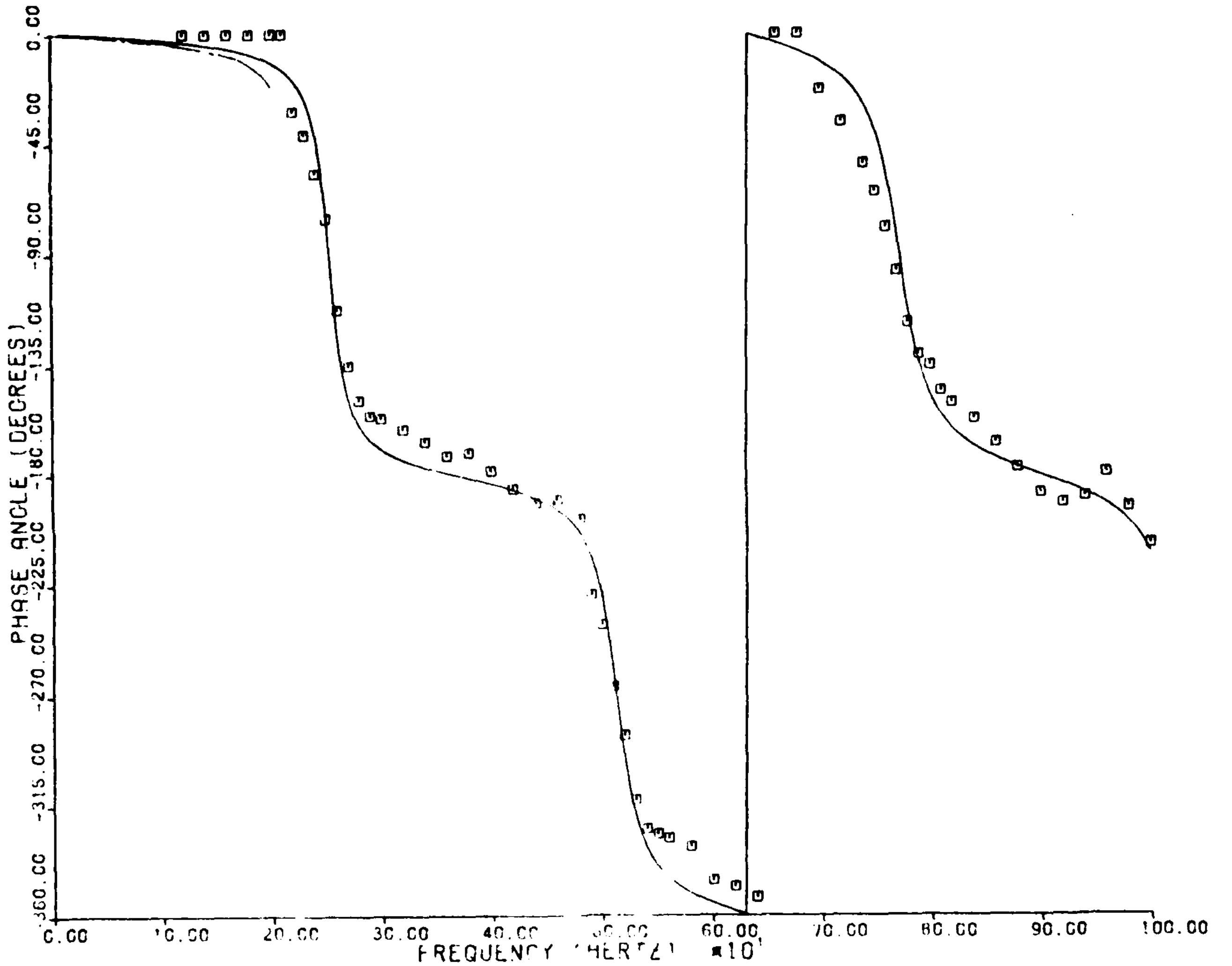

Figure 20 Experimental and Theoretical Phase vs Frequency for Case 11A

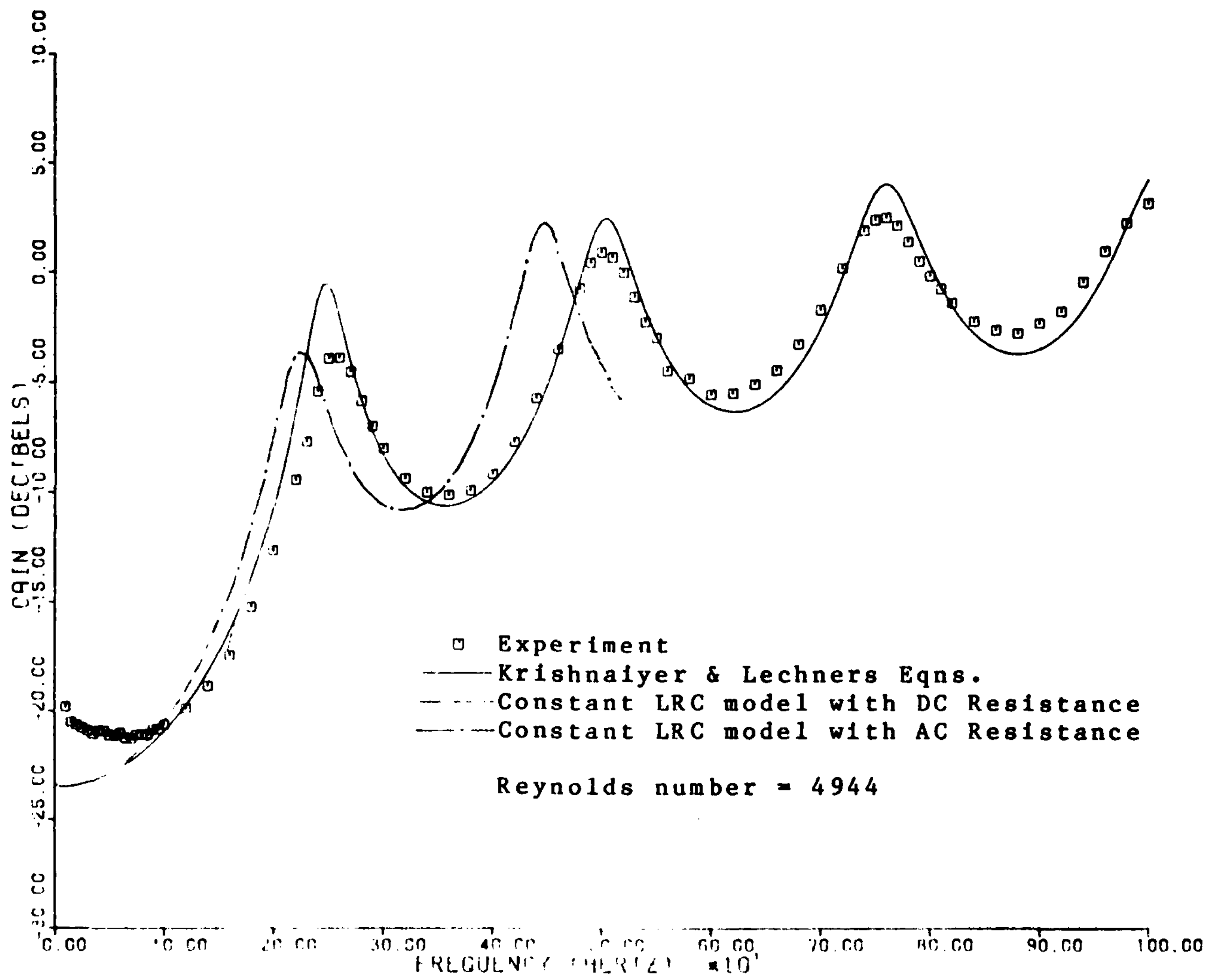

Figure 21 Experimental and Theoretical Gain vs Frequency for Case 22

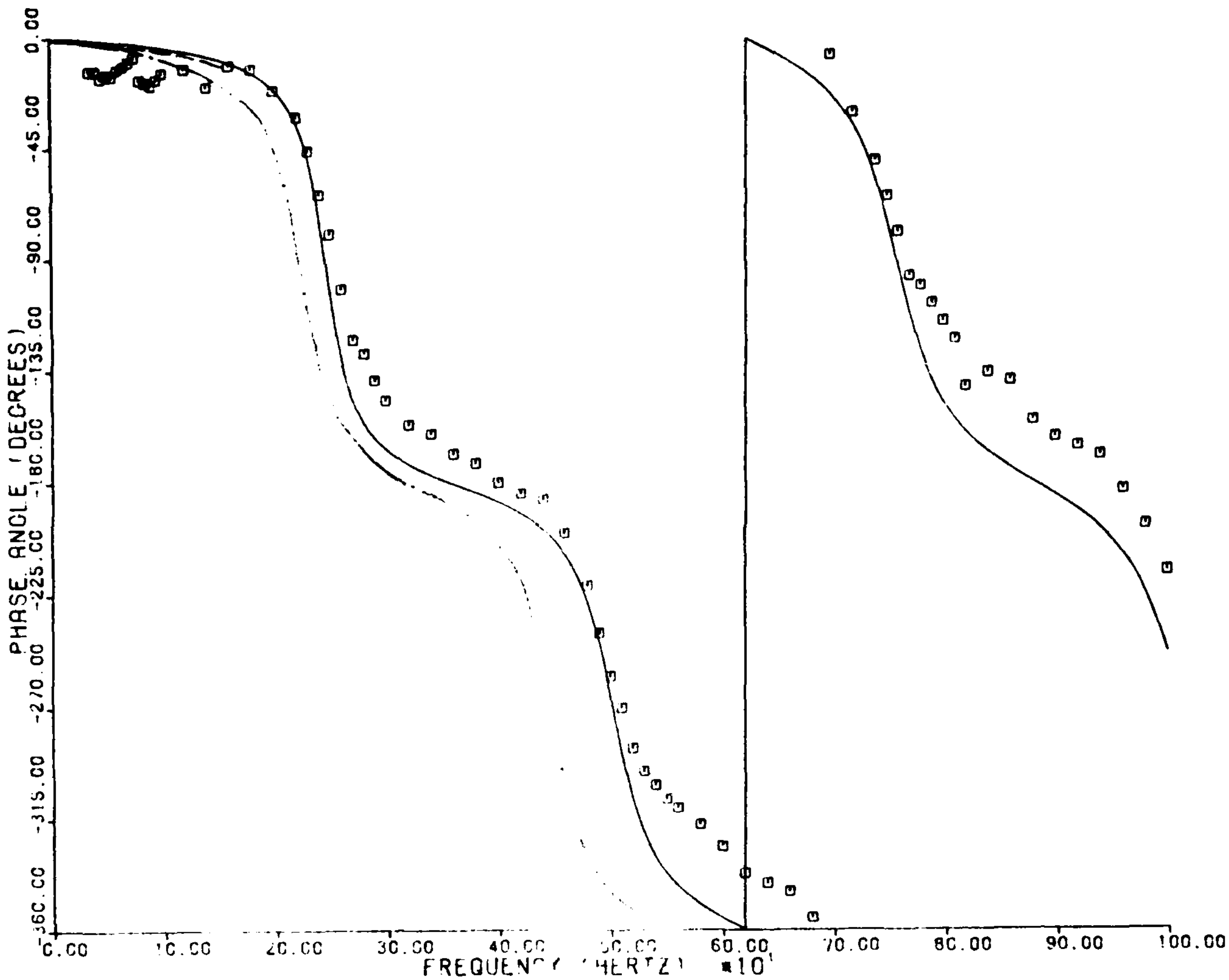

Figure 22 Experimental and Theoretical Phase vs Frequency for Case 22

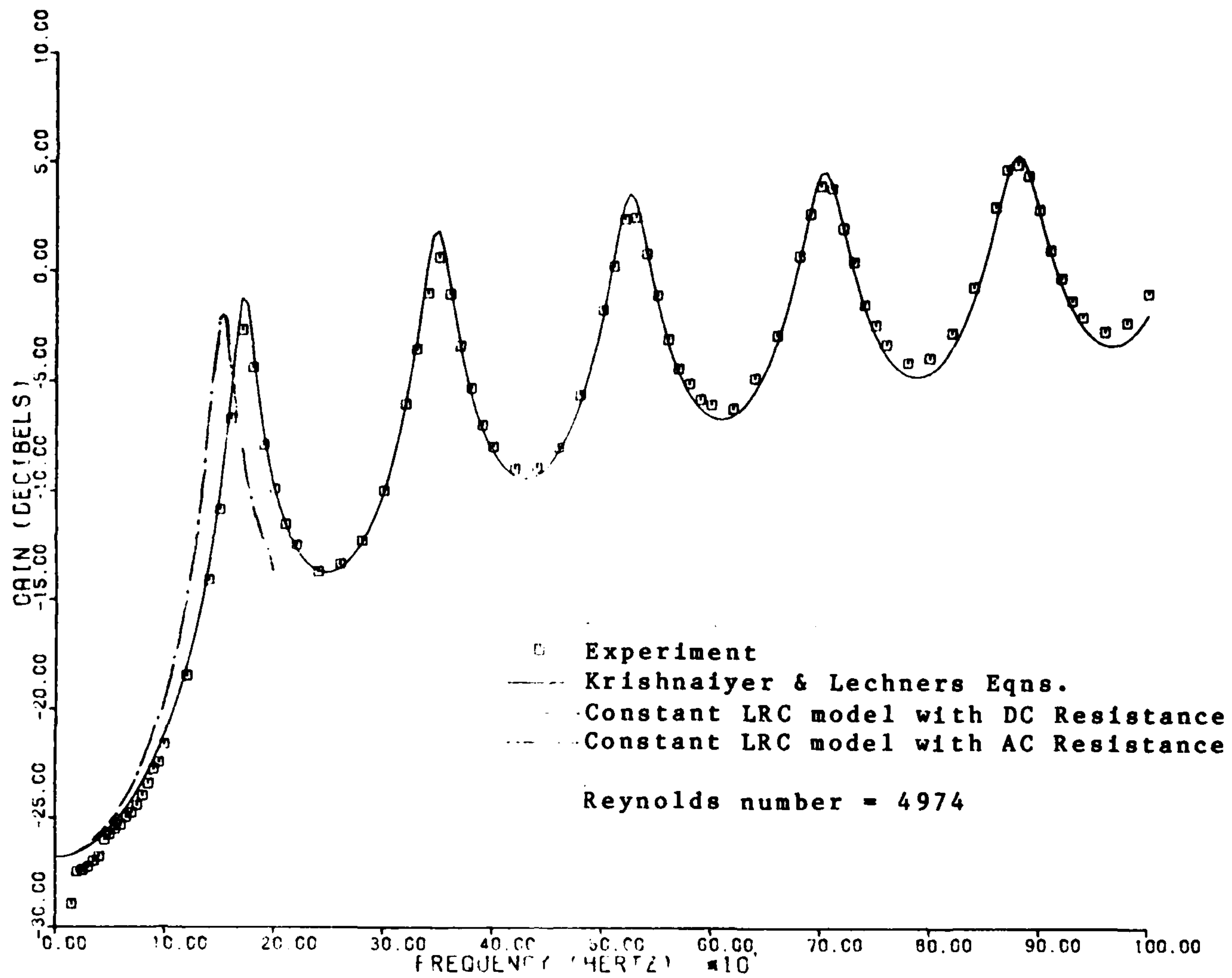

Figure 23 Experimental and Theoretical Gain vs Frequency for Case 42

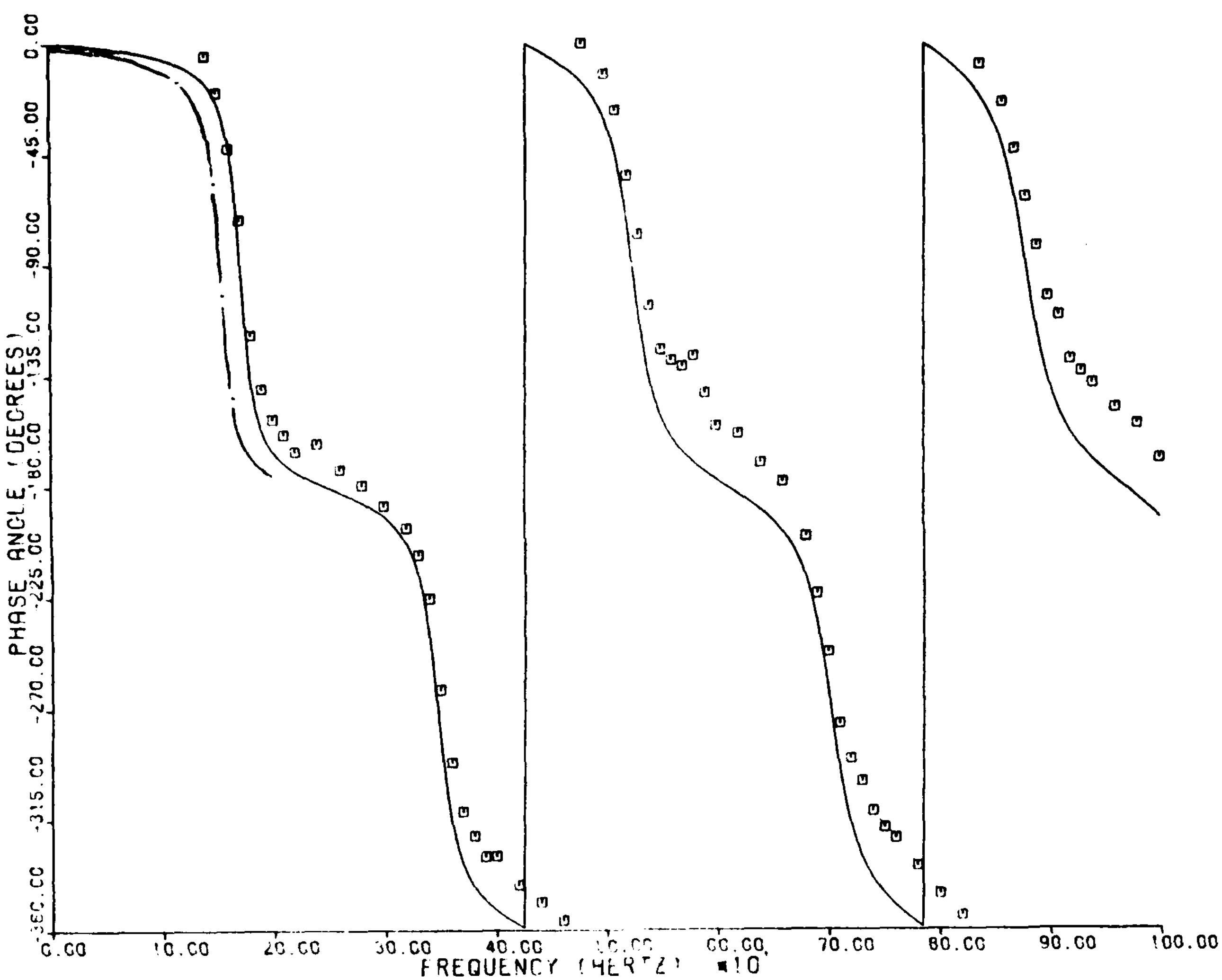

Figure 24 Experimental and Theoretical Phase vs Frequency for Case 42

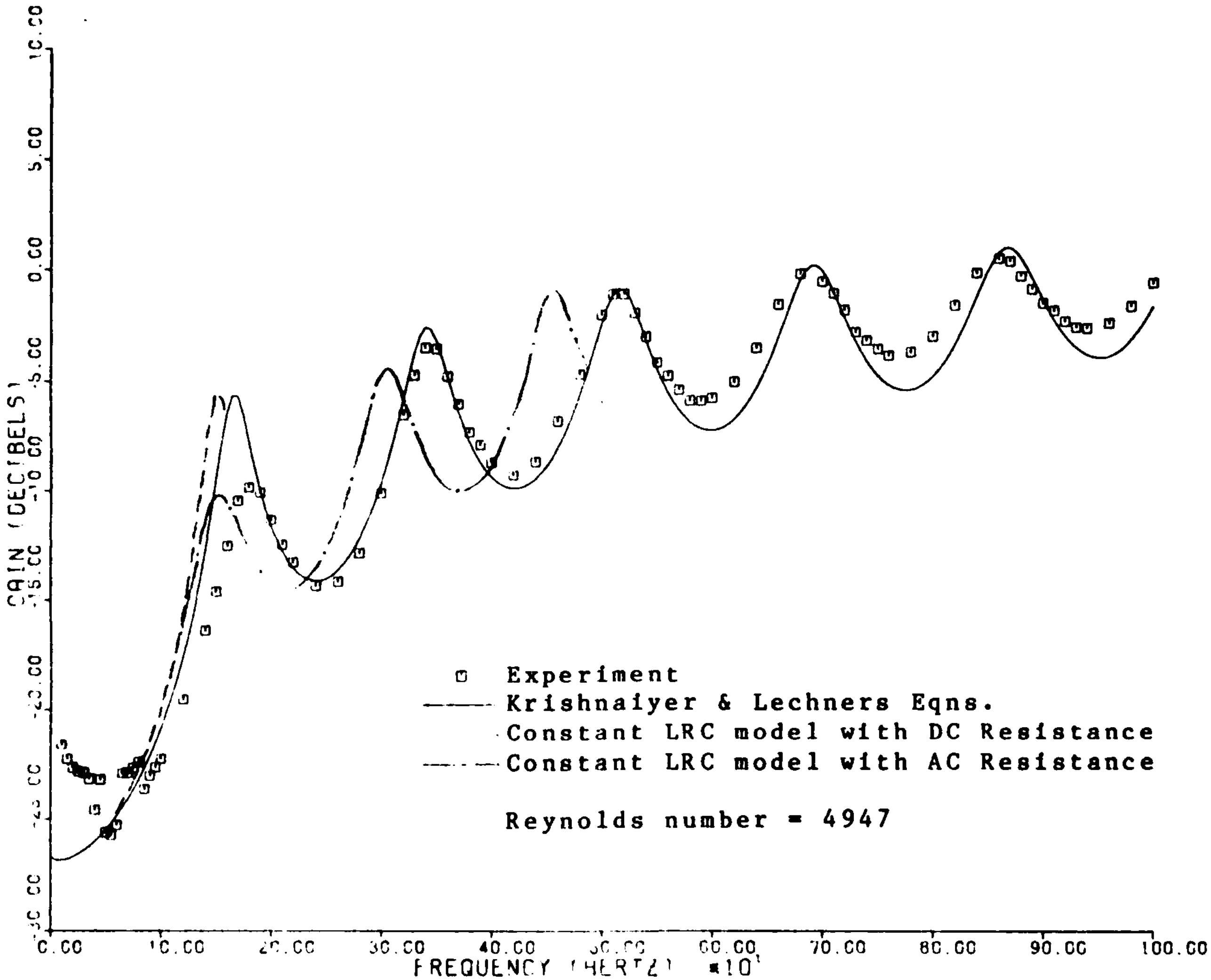

Figure 25 Experimental and Theoretical Gain vs Frequency for Case 52

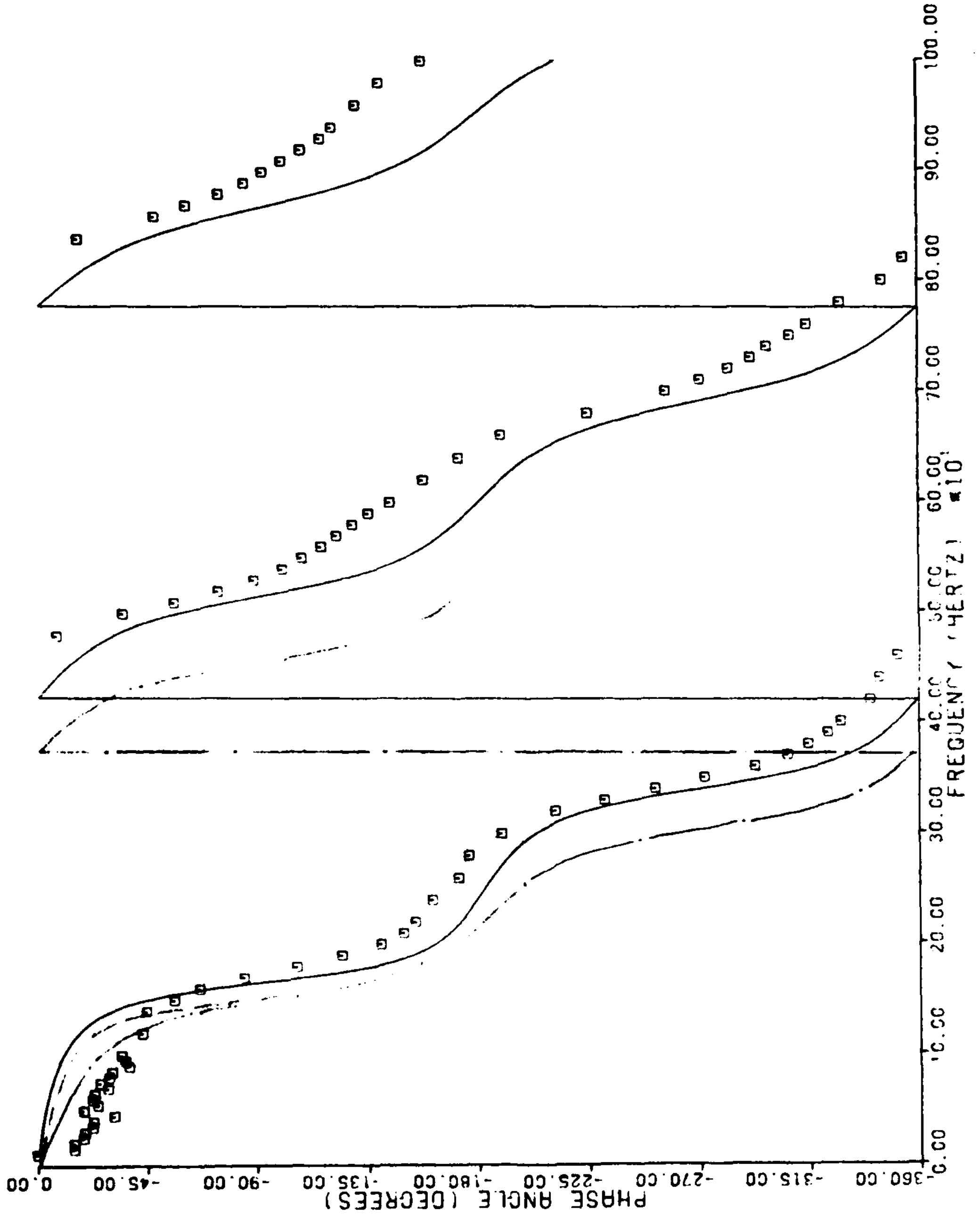

Figure 26 Experimental and Theoretical Phase vs Frequency for Case 52

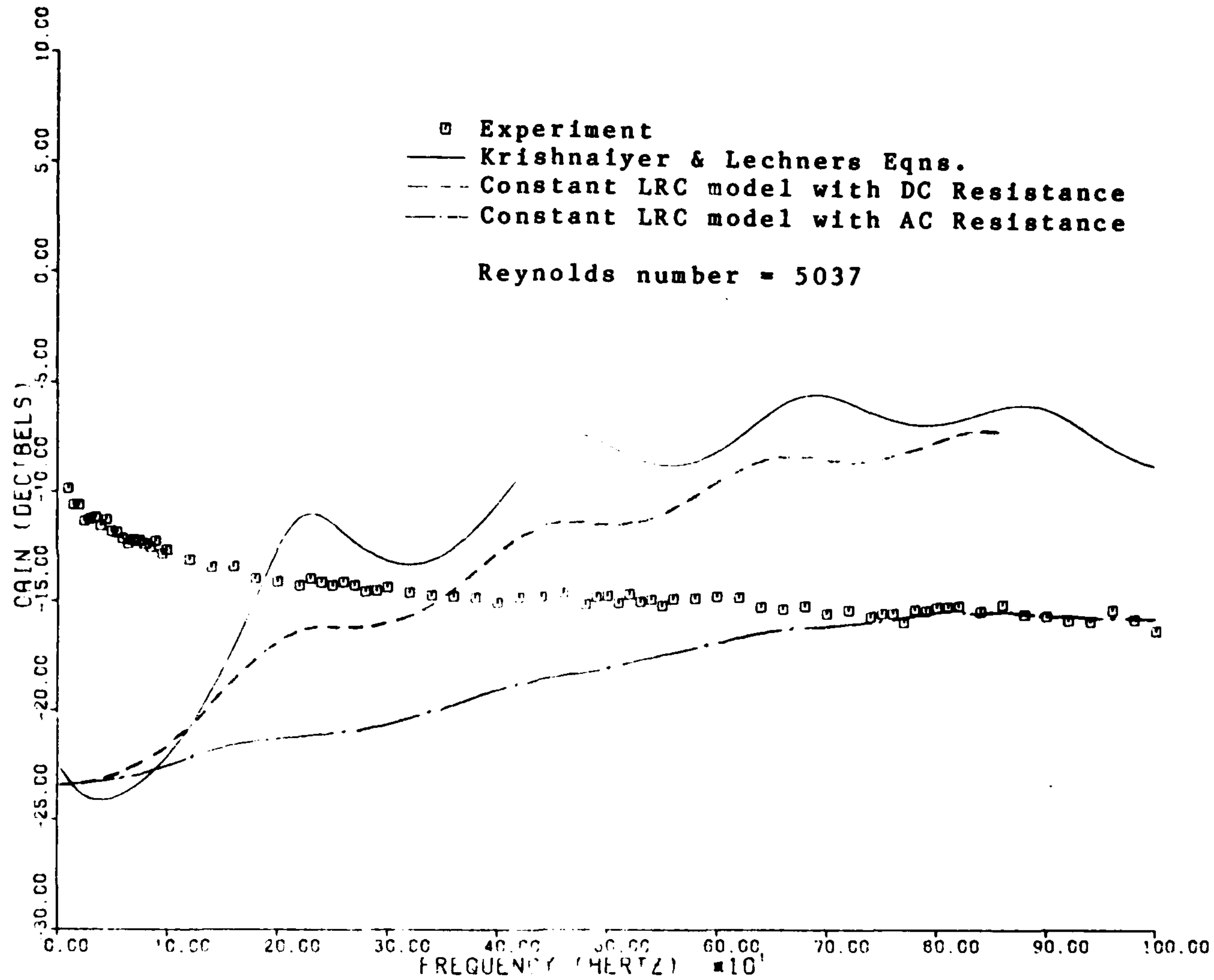

Figure 27 Experimental and Theoretical Gain vs Frequency for Case 32

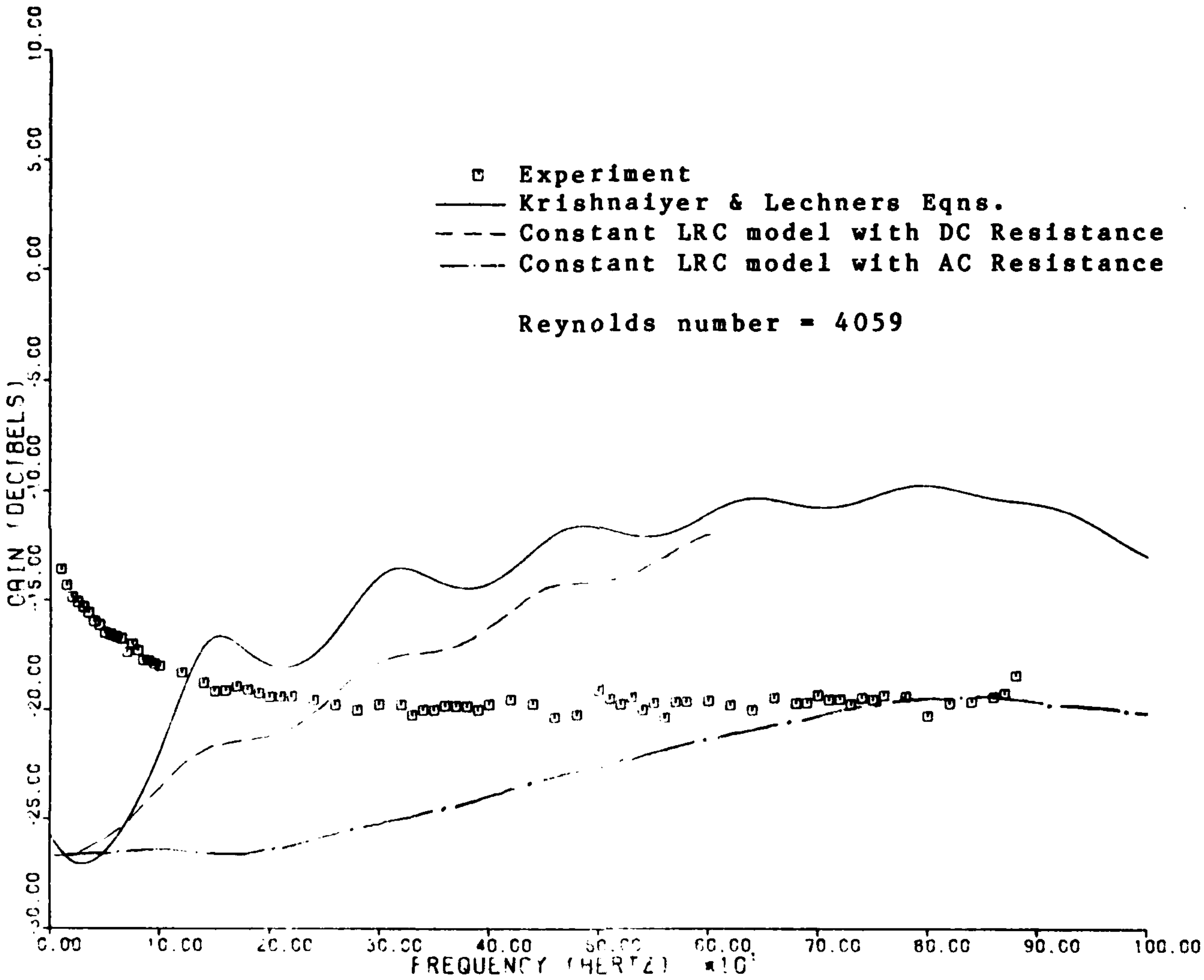

Figure 28 Experimental and Theoretical Gain vs Frequency for Case 62

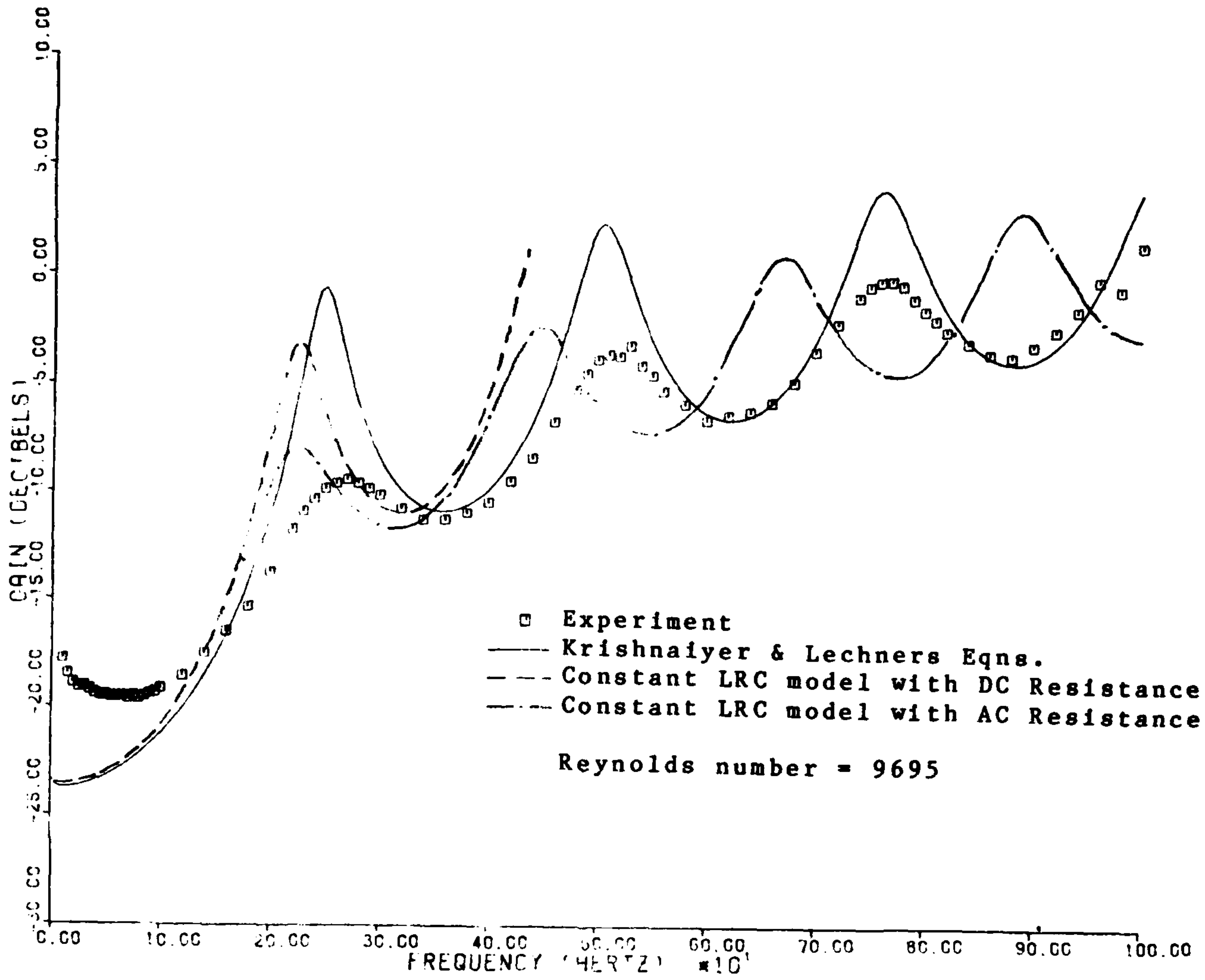

Figure 29 Experimental and Theoretical Gain vs Frequency for Case 23

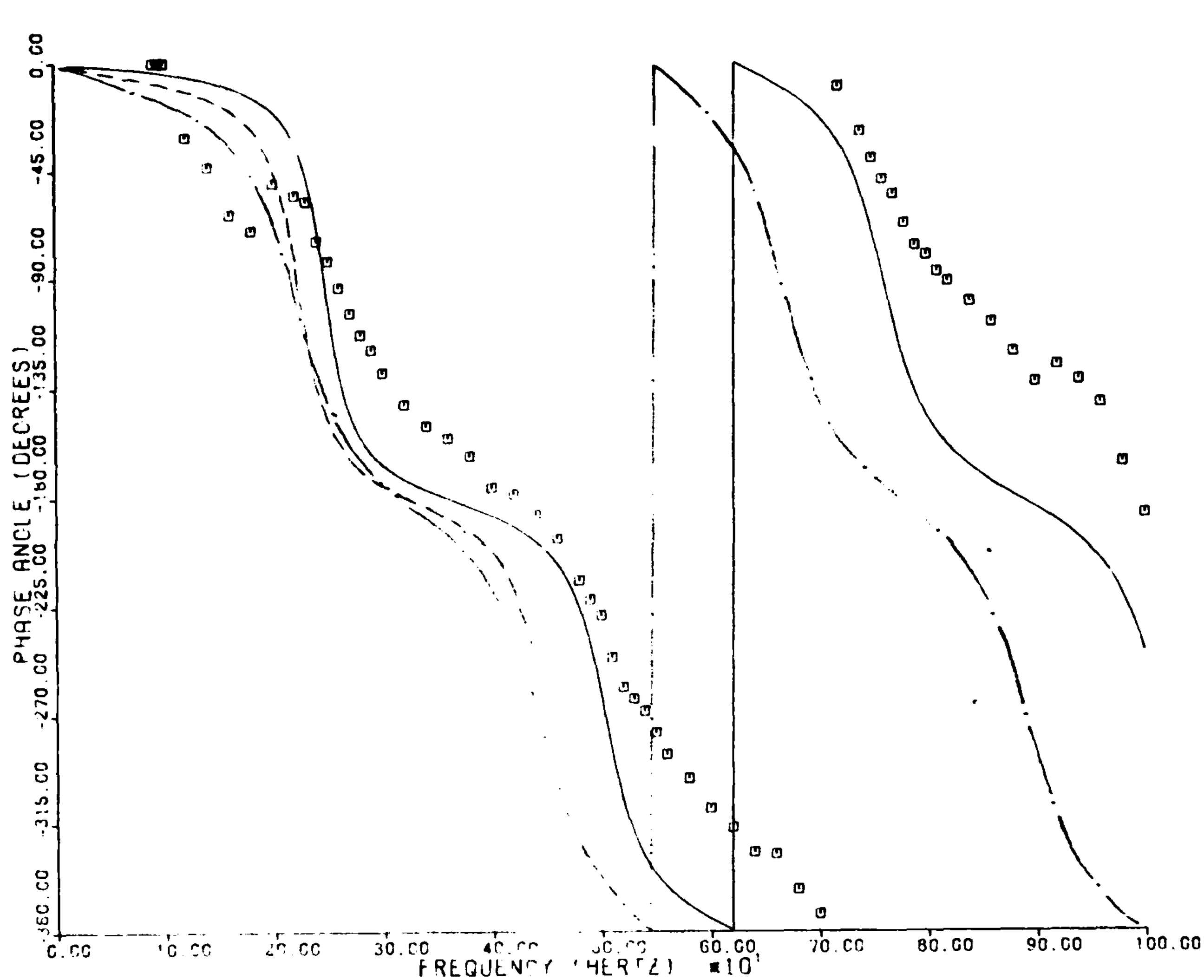

Figure 30 Experimental and Theoretical Phase vs Frequency for Case 23

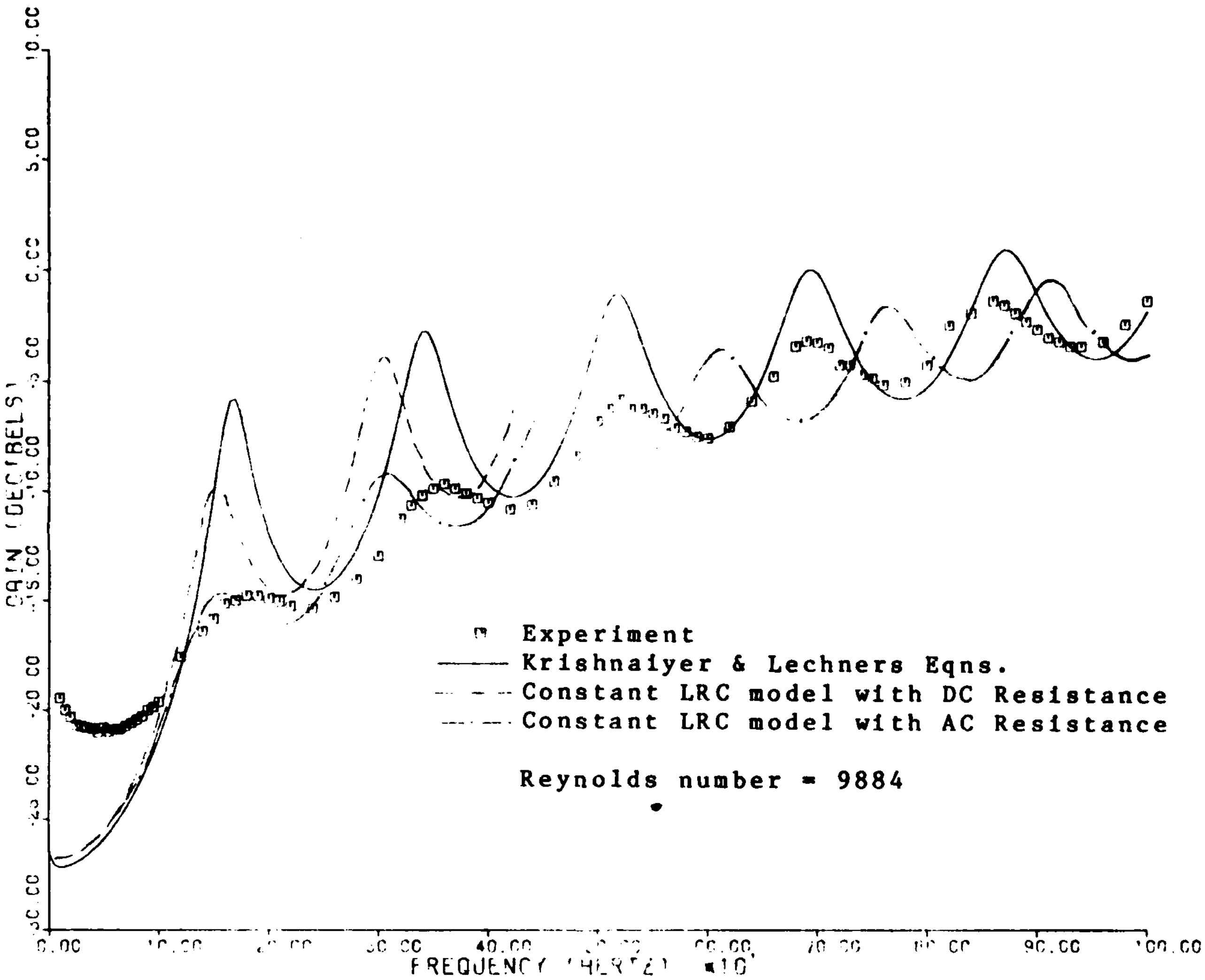

Figure 31 Experimental and Theoretical Gain vs Frequency for Case 53

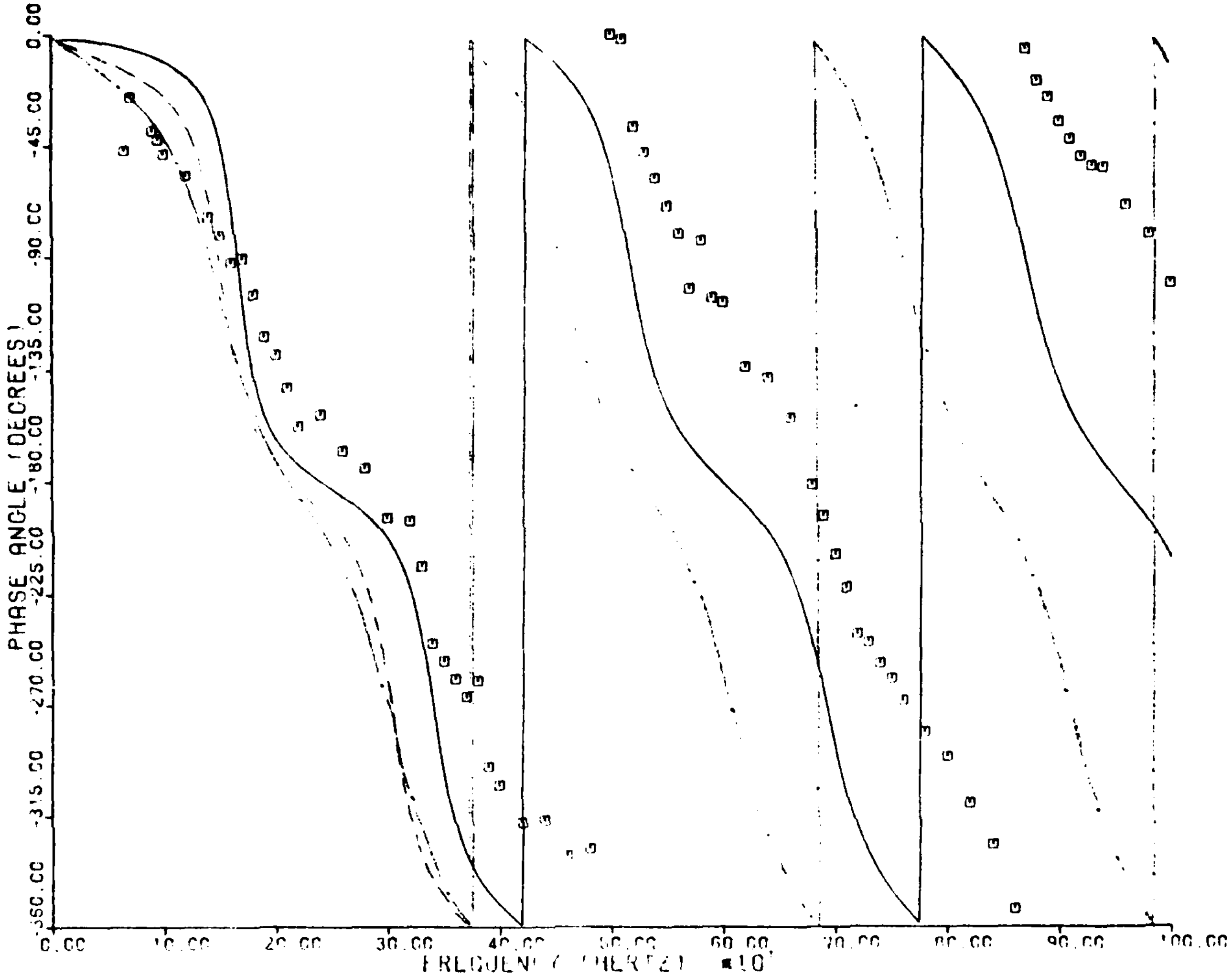

Figure 32 Experimental and Theoretical Phase vs Frequency for Case 53

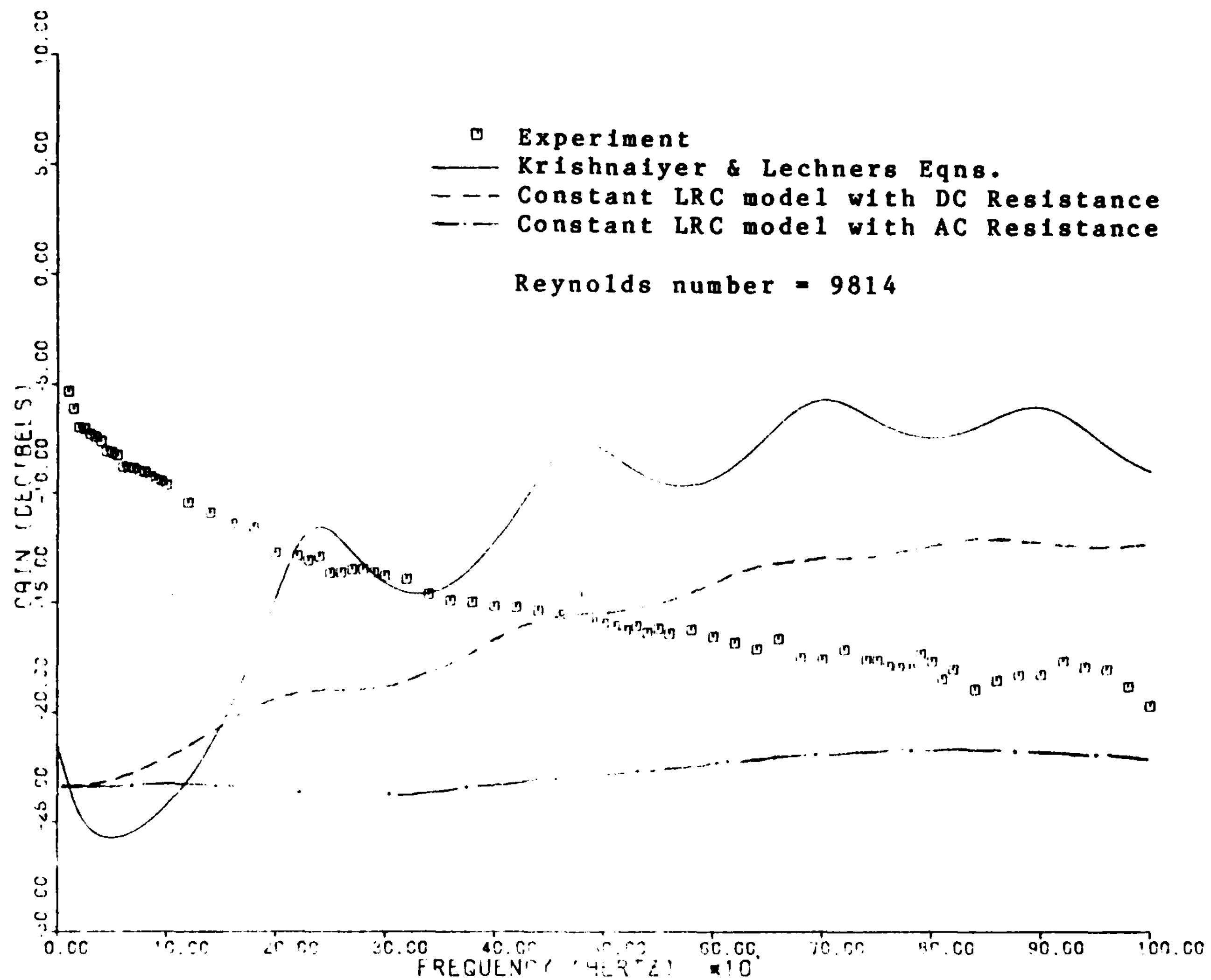

Figure 33 Experimental and Theoretical Gain vs Frequency for Case 33

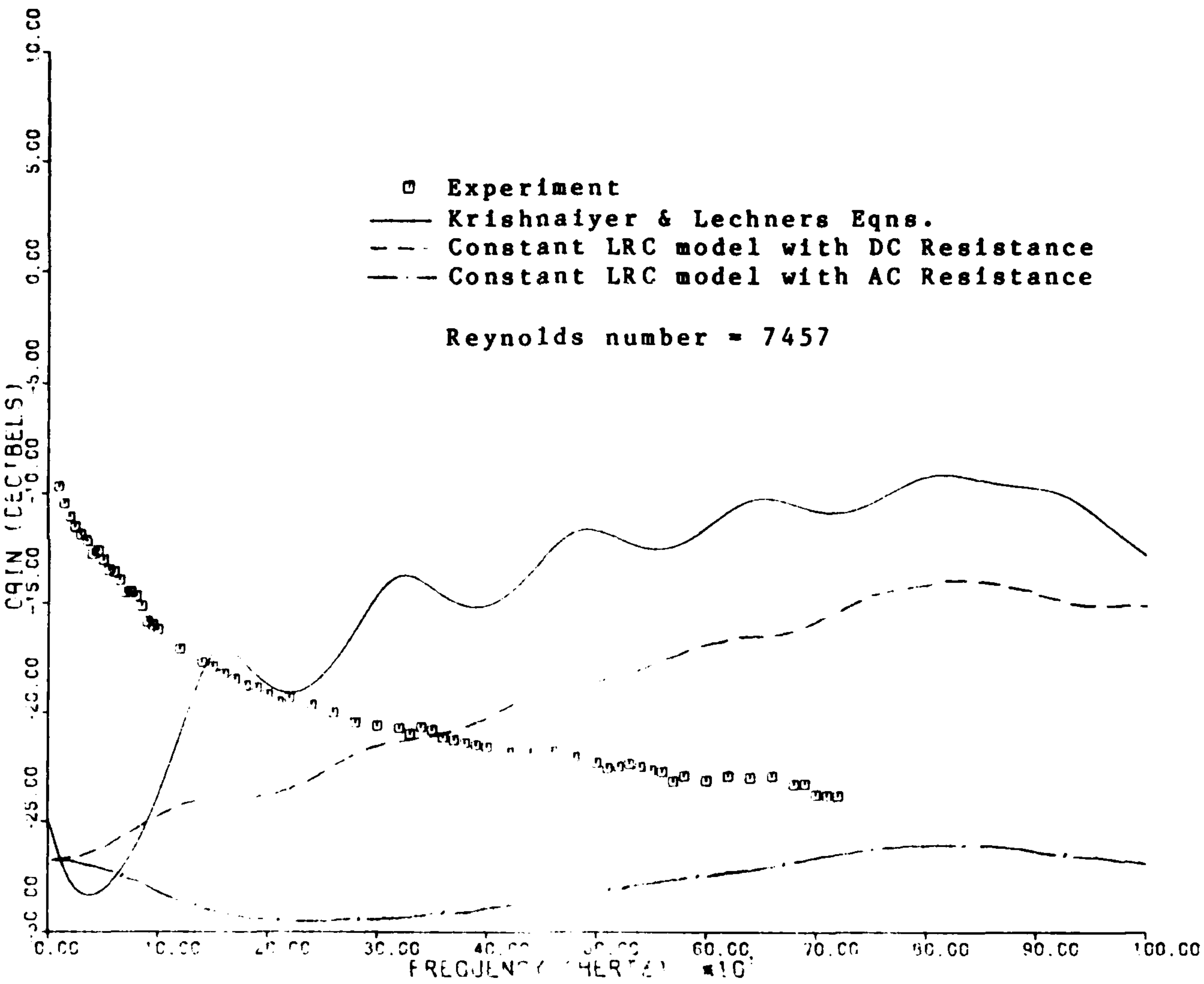

Figure 34 Experimental and Theoretical Gain vs Frequency for Case 63

are accurate for phase information for most of the lines tested.

Figures 29 and 31 best demonstrate how Krishnaiyer and Lechners equations predict attenuations which are too low. The constant LRC model with DC resistance also predicts attenuations which are too low while using the AC resistance results in much better predictions in attenuation and gain. Both of the constant LRC models are shifted on the frequency axis in the figures. The phase shift predicted is also very far off. This may be due to the assumption made in the models to use the isothermal capacitance. Moore (Ref 4) showed that the capacitance in blocked lines is isothermal at low frequencies and adiabatic at high frequencies. The author knows of no method at this time to determine the frequency dependence of the capacitance for turbulent mean flows.

Cases 33 and 63 are similar to cases 32 and 62 in that the theory does not predict the gain very well. There are very large pressure drops associated with these cases. The models were all developed for incompressible flow; this may be one of the reasons the theoretical curves are off so much. In addition, Mach numnber effects were not accounted for. There is no phase data available for these two cases because of the noise problem discussed earlier.

VI. Conclusions

1. The constant LRC model with AC resistance can accurately predict the attenuation but cannot predict the phase shift as it is used here. Because of this the model cannot be used to predict the gain because it shifts the frequency of the harmonic peaks. At this time no method exists to predict the difference in capacitance due to turbulent boundary layers. The changes in capacitance may be important in matching theoretical solutions with data.

2. The constant LRC model is most accurate when the AC resistance is used. Using the DC resistance causes the attenuation to be underestimated and prevents the model from being used to predict gain.

3. None of the models or equations used performs well in cases with large pressure drops (compressible flow).

4. The propagation characteristics of fluid transmission lines with turbulent flow exhibits laminar characteristics at high frequencies and increased attenuations at low frequencies.

VII. Recommendations

1. Studies of the effects of turbulent boundary layers on capacitance should be conducted. If possible simple models should be developed to predict the capacitance.

2. Studies on the effects of compressible flow on the propagation characteristics of fluid transmission lines should be conducted.

3. Experimental and analytical research should be conducted on the low frequency characteristics of transmission lines with turbulent mean flow.

Bibliography

1. Nichols, N. B., "The Linear Properties of Pneumatic Transmission Lines," Transactions of the Instrument Society of America, Vol. 1, 1962, pp 5-14.

2. Krishnaiyer, R. and T. J. Lechner, Jr. "An Experimental Evaluation of Fluidic Transmission Line Theory." Advances in Fluidics. Edited by F. T. Brown et al. New York: American Society of Mechanical Engineers, 1967.

3. Brown, F.T., Margolis, D.L., and Shah, R.P., "Small-Amplitude Frequency Behavior of Fluid Lines with Turbulent Flow." Journal of Basic Engineering, Trans. ASME, 91:678-693 (December 1969)

4. Moore, Ernest F. "The Small Signal Response of Fluid Transmission Lines Including Developed Mean Flow Effects." PhD dissertation. School of Engineering, Air Force Institute of Technology (AU), Wright-Patterson AFB OH, June 1977.

5. Funk, J. E. and Wood, D. J., "Frequency Response of Fluid Lines with Turbulent Flow, "Journal of Fluids Engineering, Trans. ASME, Series I, Vol. 96, No. 4, Dec. 1974, pp 365-369.

6. Franke, M. E., Private Communications. Air Force Institute of Technology, Wright-Patterson Air Force Base, OH, January 1983 - November 1983.

7. Margolis, D. L. and Brown, F. T., "Measurement of the Propagation of Long-Wavelength Disturbances Through Turbulent Flow in Tubes," Journal of Fluids Engineering, Trans. ASME, Series I, Vol. 98, No. 1, March 1976, pp. 70-78.

8. Schlichting, H., Boundary-Layer Theory, Seventh Edition, McGraw-Hill Book Company, Inc., New York, 1979.

9. Malanowski, A. J., The Dynamic Response of Fluidic Networks. MS thesis, School of Engineering, Air Force Institute of Technology (AU), Wright-Patterson AFB, OH, March 1971.

Appendix

Computer Program for the Solution of the Frequency Response of Pneumatic Transmission Lines With Turbulent Mean Flow

Computer Program Input Sequence

Basic Program

1. Read ICAS: Reads the experiment case number.

2. Read TF, PG, AMU, RE, GAM, SIG:

   TF is the line temperature in deg F
   PG is the atmospheric pressure
   AMU is the dynamic viscosity
   RE is the gas constant
   GAM is the ratio of specific heats
   SIG is the square root of the Prandtl number.

3. Read N: N is the number of lines.

4. Read DI(I), AD(I), P(I):

   DI is the line diameter
   AD is the line length
   P is the line pressure.

Calcomp Plotter Subroutine

5. Read CASE(I): CASE same as ICAS.

6. Read NPTS, LSMB:

   NPTS is the number of experimental input points
   LSMB is the plotter symbol used to represent the experimental data

7. Read FREQ, PS, PR, PHT

   FREQ is the experimental frequency at which the data was recorded.
   PS is the RMS voltage of the sending dynamic transducer
   PR is the RMS voltage of the recieving dynamic transducer
   PHT is the phase lag between the sending and recieving ports in milliseconds.

```
      PROGRAM MSB(INPUT,OUTPUT,TAPE5=INPUT,TAPE6=OUTPUT,TAPE7,TAPE9)
C
C     TRANSMISSION LINE STUDY/Z-IN METHOD WITH BRANCH    SHORT OUTPUT
      DIMENSION DBT(300),DI(100),AD(100),AR(100),CV(100),RVT(100),
     1OMT(100),CNA(100),GMA(100),AGM(100),FN(100),RN(100),GN(100),
     2ALN(100),CN(100),AN(100),BTN(100),AMC(100),AZRN(100),BZRN(100),
     3AZIN(100),BZIN(100),DC(100),DG(100),DD(100),P(100),RHO(100),
     4ANU(100),CA(100),QTCA(100),OMG(300),RTP(100),GP(100),BETA(100),
     5AZOT(100),BZOT(100),REY(100),Q(100),BET(100),TURB(100)
      DIMENSION DB(300),OMGX(300),OMGP(300),PHASE(300),PH(300),CASE(100)
      DATA PI/3.1415926/
      DATA TPI/6.2831853/
C***********************************************************************
C***********************************************************************
C***********************************************************************
      CALL PLOTS(0.,0.,9)
1     READ(5,*)ICAS
 110  READ(5,*)TF,PG,AMU,RE,GAM,SIG
      READ(5,*) N
C
C    *******************************************************************
C     AD IS THE LINE LENGTH
C     DI IS THE LINE DIAMETER
C     P IS THE INLET PRESSURE
C     A ONE FOR NLINE OR MLINE INDICATES THE LINE IS OPEN AND ANY OTHER
C     NUMBER INDICATES A BLOCKED END.
C    *******************************************************************
C
      DO 898 I=1,N
      READ(5,*) DI(I),AD(I),P(I)
 898  CONTINUE
      NPG=0
      ICT=1
      IND=1
      NNN=1
      M=0
C*****************************************************************
C     DETERMINE REYNOLDS NUMBER FOR LINE
      TOTL=0.0
      DO 2 I=3,N
      TOTL=TOTL+AD(I)
  2   CONTINUE
      RHO(N)=(PG+P(N))/(RE*(TF+460))
      REYT=(PG*P(N)+.5*(P(N)**2.))*(DI(N)**3.)/32./AMU/AMU
      REYT=REYT/TOTL/RE/(TF+460.)
      IF (REYT.LT.2300.) GOTO 3
      REYT=(REYT*32./.1582)**(4./7.)
  3   QM=REYT*PI*DI(N)*AMU/4.
      DO 23 I=1,N
      PBR=P(I)+PG
      TBR=TF+460.
      RHO(I)=PBR/(RE*TBR)
      ANU(I)=AMU/RHO(I)
```

```
      CA(I)=SQRT(PBR*GAM/RHO(I))
      AR(I)=PI*DI(I)*DI(I)/4.
      CV(I)=(8.*PI*ANU(I))/AR(I)
      OMT(I)=CV(I)/(SIG*SIG)
      CNA(I)=(8.*PI*AMU)/(AR(I)*AR(I))
      Q(I)=QM/RHO(I)
23    CONTINUE
      Q(1)=0.0
      Q(2)=0.0
      GMN1=.5*(GAM-1.)
      DO 26 I=1,N
      REY(I)=(4.*RHO(I)*Q(I))/(PI*DI(I)*AMU)
      PBR=P(I)+PG
      TEMP=GMN1/(GAM*PBR)
      GMA(I)=TEMP*AR(I)
      AGM(I)=AR(I)/(GAM*PBR)
      QTCA(I)=0.25*CA(I)
      RVT(I)=.3164*AMU/2./AR(I)/DI(I)/DI(I)
      RVT(I)=RVT(I)*(REY(I)**.75)
 26   FN(I)=QTCA(I)/AD(I)
      NST=1
      DW=0.
      Y=1.
40    DO 80 J=1,NST
      M=M+1
      Y=Y+DW
      W=TPI*Y
      DO 27 I=1,N
      ARG=.5*SQRT(W/CV(I))
27    RN(I)=CNA(I)*(.375+ARG+(.375/(4.*ARG)))
      DO 28 I=1,N
      DC(I)=.25+SQRT(W/OMT(I))+.125*SQRT(OMT(I)/W)
      DG(I)=SQRT(W/OMT(I))-.125*SQRT(OMT(I)/W)
      DD(I)=DC(I)*DC(I)+DG(I)*DG(I)
28    GN(I)=W*(GAM-1.)*AGM(I)*DG(I)/DD(I)
      DO 29 I=1,N
      ARG=.5*SQRT(CV(I)/W)
  29  ALN(I)=RHO(I)*(1.+ARG-(ARG*(15.*CV(I)/(W*64.))))/AR(I)
      TEMP=GMN1/W
      DO 30 I=1,N
      TURB(I)=0
30    CN(I)=AGM(I)*(1.+((GAM-1.)*DC(I)/DD(I)))
      TEMP=-W*W
      DO 31 I=1,N
      TEM1=RN(I)*GN(I)+TEMP*ALN(I)*CN(I)
      TEM2=W*(RN(I)*CN(I)+GN(I)*ALN(I))
      CALL RTCMP(ARG1,ARG2,TEM1,TEM2)
      AN(I)=ARG1
      BTN(I)=ARG2
      TEM1=-W*W*RHO(I)/(P(I)+PG)
      TEM2=W*AR(I)*RVT(I)/(P(I)+PG)
      CALL RTCMP(ARG1,ARG2,TEM1,TEM2)
      TAN=ARG1
```

```
      TBTN=ARG2
      IF(AN(I).GE.TAN) GO TO 31
      AN(I)=TAN
      BTN(I)=TBTN
      TURB(I)=1
 31   AMC(I)=TPI/BTN(I)
C     CALCULATE ZO
      DO 32 I=1,N
      TEM1=W*ALN(I)
      TEM2=W*CN(I)
      TEM3=RN(I)
      TEM4=GN(I)
      CALL CMPDV(ARG1,ARG2,TEM3,TEM1,TEM4,TEM2)
      CALL RTCMP(AZRNI,BZRNI,ARG1,ARG2)
      AZRN(I)=AZRNI
      BZRN(I)=BZRNI
      IF(TURB(I).EQ.0) GO TO 32
      TEM1=RHO(I)*(P(I)+PG)/AR(I)/AR(I)
      TEM2=-RVT(I)*(P(I)+PG)/W/AR(I)
      CALL RTCMP(ARG1,ARG2,TEM1,TEM2)
      AZRN(I)=ARG1
      BZRN(I)=ARG2
  32  CONTINUE
C CALCULATE Z IN 1
      I=1
      TEMP=AN(I)*AD(I)
      IF(TEMP.GT.88.) GO TO 80
      ARG1=COSH(TEMP)
      ARG2=SINH(TEMP)
      TEM5=BTN(I)*AD(I)
      TEMP=COS(TEM5)
      TEM1=ARG1*TEMP
      TEM3=ARG2*TEMP
      TEMP=SIN(TEM5)
      TEM2=ARG2*TEMP
      TEM4=ARG1*TEMP
      CALL CMPDV(ARG1,ARG2,TEM1,TEM2,TEM3,TEM4)
      TEM1=AZRN(I)
      TEM2=BZRN(I)
      CALL CMPMP(TEM3,TEM4,TEM1,TEM2,ARG1,ARG2)
      AZIN(I)=TEM3
      BZIN(I)=TEM4
C CALCULATE Z IN 3
      I=3
      TEM1=AZRN(I)
      TEM2=BZRN(I)
      TEM3=0.
      TEM4=0.
      TEM5=AN(I)
      TEM6=AD(I)
      TEM7=BTN(I)
      CALL CALZIN(AARG,BARG,TEM1,TEM2,TEM3,TEM4,TEM5,TEM6,TEM7)
      AZIN(I)=AARG
```

```
      BZIN(I)=BARG
C CALCULATE Z IN 4,5
      DO 34 I=4,5
      TEM1=AZRN(I)
      TEM2=BZRN(I)
      TEM3=AZIN(I-1)
      TEM4=BZIN(I-1)
      TEM5=AN(I)
      TEM6=AD(I)
      TEM7=BTN(I)
      CALL CALZIN(AARG,BARG,TEM1,TEM2,TEM3,TEM4,TEM5,TEM6,TEM7)
      AZIN(I)=AARG
   34 BZIN(I)=BARG
C CALCULATE Z IN 2
      I=2
      TEM1=AZRN(I)
      TEM2=BZRN(I)
      TEM3=AZIN(I-1)
      TEM4=BZIN(I-1)
      TEM5=AN(I)
      TEM6=AD(I)
      TEM7=BTN(I)
      CALL CALZIN(AARG,BARG,TEM1,TEM2,TEM3,TEM4,TEM5,TEM6,TEM7)
      AZIN(I)=AARG
      BZIN(I)=BARG
C CALCULATE RECEIVING Z FOR LINE 6
      I=6
      TEM1=AZIN(I-1)
      TEM2=BZIN(I-1)
      TEM3=AZIN(I-4)
      TEM4=BZIN(I-4)
      CALL ZEBRA(AZOTI,BZOTI,TEM1,TEM2,TEM3,TEM4)
      AZOT(I)=AZOTI
      BZOT(I)=BZOTI
C CALCULATE Z IN 6 INCLUDING R-TRANSDUCER
      TEM1=AZRN(I)
      TEM2=BZRN(I)
      TEM3=AN(I)
      TEM4=AD(I)
      TEM5=BTN(I)
      CALL CALZIN(AZINI,BZINI,TEM1,TEM2,AZOTI,BZOTI,TEM3,TEM4,TEM5)
      AZIN(I)=AZINI
      BZIN(I)=BZINI
C CALCULATE Z IN 7, 8, 9, AND 10 INCLUDING R-TRANSDUCERS
      DO 39 I=7,10
      TEM1=AZRN(I)
      TEM2=BZRN(I)
      TEM3=AZIN(I-1)
      TEM4=BZIN(I-1)
      TEM5=AN(I)
      TEM6=AD(I)
      TEM7=BTN(I)
      CALL CALZIN(AZINI,BZINI,TEM1,TEM2,TEM3,TEM4,TEM5,TEM6,TEM7)
```

```
      AZIN(I)=AZINI
   39 BZIN(I)=BZINI
C CALCULATE P5/P6 INCLUDING R-TRANSDUCER
      I=6
      TEMP=BTN(I)*AD(I)
      CSBI1=COS(TEMP)
      SNBI1=SIN(TEMP)
      TEMP=AN(I)*AD(I)
      ARG1=COSH(TEMP)
      ARG2=SINH(TEMP)
      TEM1=ARG1*CSBI1
      TEM2=ARG2*SNBI1
      AZOTI=AZOT(I)
      BZOTI=BZOT(I)
      AZINI=AZIN(I)
      BZINI=BZIN(I)
      CALL CMPDV(TEM7,TEM8,AZOTI,BZOTI,AZINI,BZINI)
      CALL CMPMP(TEM3,TEM4,TEM7,TEM8,TEM1,TEM2)
      TEM5=ARG2*CSBI1
      TEM6=ARG1*SNBI1
      TEM9=AZRN(I)
      TEM10=BZRN(I)
      CALL CMPDV(TEM7,TEM8,AZOTI,BZOTI,TEM9,TEM10)
      CALL CMPMP(TEM1,TEM2,TEM7,TEM8,TEM5,TEM6)
      TEM1=TEM3-TEM1
      TEM2=TEM4-TEM2
      TEMP=TEM1*TEM1+TEM2*TEM2
      BETA(I)=ATAN2(TEM2,TEM1)
      BET(I)=(180./PI)*BETA(I)
      RTP(I-1)=SQRT(TEMP)
      GP(I-1)=20.*ALOG10(RTP(I-1))
C CALCULATE P6/P7, P7/P8, P8/P9, AND P9/P10 INCLUDING R-TRANSDUCER
      DO 43 I=7,10
      TEMP=BTN(I)*AD(I)
      CSBI1=COS(TEMP)
      SNBI1=SIN(TEMP)
      TEMP=AN(I)*AD(I)
      ARG1=COSH(TEMP)
      ARG2=SINH(TEMP)
      TEM1=ARG1*CSBI1
      TEM2=ARG2*SNBI1
      AZINI1=AZIN(I-1)
      BZINI1=BZIN(I-1)
      AZINI=AZIN(I)
      BZINI=BZIN(I)
      CALL CMPDV(TEM7,TEM8,AZINI1,BZINI1,AZINI,BZINI)
      CALL CMPMP(TEM3,TEM4,TEM7,TEM8,TEM1,TEM2)
      TEM5=ARG2*CSBI1
      TEM6=ARG1*SNBI1
      TEM9=AZRN(I)
      TEM10=BZRN(I)
      CALL CMPDV(TEM7,TEM8,AZINI1,BZINI1,TEM9,TEM10)
      CALL CMPMP(TEM1,TEM2,TEM7,TEM8,TEM5,TEM6)
```

```
      TEM1=TEM3-TEM1
      TEM2=TEM4-TEM2
      TEMP=TEM1*TEM1+TEM2*TEM2
      BETA(I)=ATAN2(TEM2,TEM1)
      BET(I)=(180./PI)*BETA(I)
      RTP(I-1)=SQRT(TEMP)
   43 GP(I-1)=20.*ALOG10(RTP(I-1))
      RTPT=RTP(5)*RTP(6)*RTP(7)*RTP(8)*RTP(9)
      GPT=20.*ALOG10(RTPT)
      BETAR=BETA(6)+BETA(7)+BETA(8)+BETA(9)+BETA(10)
   35 IF (BETAR.LE.0.) GOTO 36
      BETAR=BETAR-TPI
      GOTO 35
   36 IF (BETAR.GT.-TPI) GOTO 37
      BETAR=BETAR+TPI
      GOTO 36
   37 BETAD=(180./PI)*BETAR
      WRITE(6,700)Y,BETAD,RTPT,GPT
  700 FORMAT(2X,6HFREQ =,F7.0,3X,11HBETA(DEG) =,F7.2,5X,6HGAIN =,
     11PE12.4,1X,2HOR,1X,1PE12.4,2HDB)
      DBT(M)=GPT
      OMG(M)=Y
      PHASE(M)=BETAD
      IF(NNN.GT.1) GO TO 80
      WRITE(6,810)
  810 FORMAT(1H0,13X,6HLENGTH,9X,8HDIAMETER,7X,8HPRESSURE,9X,5HC ADB,10X
     1,3HFN , 7X,7HDENSITY,5X,11HREYNOLDS NO)
  802 FORMAT(1H0,1X,5HLINE ,I2,3X, 8(1PE12.4,2X))
      DO 803 I=1,N
  803 WRITE(6,802)I,AD(I),DI(I),P(I),CA(I),FN(I),RHO(I),REY(I)
      NNN=2
80    CONTINUE
      GO TO (85,611),IND
85    Y=0.
      DW=5.
      NST=200
      IND=2
      GO TO 40
C
C   *********************************************************************
C   *********************************************************************
C   *********************************************************************
C   *********************************************************************
C   *********************************************************************
C   *********************************************************************
C   *********************************************************************
C         THIS SECTION IS FOR THE CALCOMP PLOTTER.  ONE SET OF
C         EXPERIMENTAL DATA MUST BE INCLUDED WITH EACH RUN.
C
C     NPTS IS THE NUMBER OF EXPERIMENTAL POINTS TO BE INPUT.
C     LSMB IS THE PLOTTER SYMBOL TO BE USED FOR GPX AND PHD.
C     SEE A CALCOMP PLOTTER USERS MANUAL FOR DESCRIPTION.
C     FREQ,PS,PR, AND PHD ARE THE INPUT EXPERIMENTAL VALUES.
```

```
C
C**********
C
611   IF(ICAS)502,502,610
610   CALL FACTOR(0.625)
      OMG(M+1)=0.
      OMG(M+2)=100.
      DBT(M+1)=-30.
      DBT(M+2)=5.0
      CALL AXIS(0.,0.,17HFREQUENCY (HERTZ),-17,10.0,0.,OMG(M+1),
     +OMG(M+2))
      CALL AXIS(0.,0.,15HGAIN (DECIBELS),15,8.,90.,DBT(M+1),
     +DBT(M+2))
      CALL LINE(OMG,DBT,M,1,0,4)
204   FORMAT(6X,1A2)
      READ(7,204)CASE(1)
      READ(7,*)NPTS,LSMB
      WRITE(6,207)
207   FORMAT(1H0,10X,1HN,4X,4HFREQ,10X,2HPS,10X,2HPR,10X,4HGAIN,10X,
     +5HPHASE)
      J=0
      DO 69 I=1,NPTS
612   READ(7,*)FREQ,PS,PR,PHT
      GPX=20.*ALOG10(PR/PS)
      PHD=-PHT*FREQ*.36
      WRITE(6,209)I,FREQ,PS,PR,GPX,PHD
209   FORMAT(7X,I5,5F12.5)
      DB(I)=GPX
      OMGX(I)=FREQ
      IF(PHD.GT.0) GOTO 69
      J=J+1
      PH(J)=PHD
      OMGP(J)=FREQ
      JMAX=J
   69 CONTINUE
      OMGX(NPTS+1)=OMG(M+1)
      DB(NPTS+1)=DBT(M+1)
      OMGX(NPTS+2)=OMG(M+2)
      DB(NPTS+2)=DBT(M+2)
      CALL LINE(OMGX,DB,NPTS,1,-1,LSMB)
      CALL PLOT(15.0,0,-3)
      CALL FACTOR(0.625)
      OMG(M+1)=0.
      OMG(M+2)=100.
      PHASE(M+1)=-360.
      PHASE(M+2)=45.
      CALL AXIS(0.,0.,17HFREQUENCY (HERTZ),-17,10.,0.,OMG(M+1),
     +OMG(M+2))
      CALL AXIS(0.,0.,21HPHASE ANGLE (DEGREES),21,8.,90.,PHASE(M+1),
     +PHASE(M+2))
      CALL LINE(OMG,PHASE,M,1,0,4)
      OMGP(JMAX+1)=OMG(M+1)
      OMGP(JMAX+2)=OMG(M+2)
```

```
      PH(JMAX+1)=PHASE(M+1)
      PH(JMAX+2)=PHASE(M+2)
      CALL LINE(OMGP,PH,JMAX,1,-1,LSMB)
      CALL SYMBOL(15.,5.,.165,5HCASE ,0.,5)
      CALL SYMBOL(16.,5.,.165,CASE(1),0.,2)
 1003 CALL PLOT(10.0,0,-3)
C    *********************************************************************
C    *********************************************************************
C    *********************************************************************
C
501   CALL PLOTE
502   STOP
      END
C CALCULATES ROOT OF A COMPLEX NUMBER
      SUBROUTINE RTCMP(X,Y,A,B)
      CALL ANGL(TEMP,A,B)
      TEMP=.5*TEMP
      Y=A*A+B*B
      X=SQRT(Y)
      X=SQRT(X)
      Y=X*SIN(TEMP)
      X=X*COS(TEMP)
      RETURN
      END
C MULTIPLIES TWO COMPLEX NUMBERS
      SUBROUTINE CMPMP(X,Y,A1,A2,B1,B2)
      X=A1*B1-A2*B2
      Y=A1*B2+A2*B1
      RETURN
      END
C FINDS THE QUOTIENT OF TWO COMPLEX NUMBERS
      SUBROUTINE CMPDV(C1,C2,A1,A2,B1,B2)
      TEMP=B1*B1+B2*B2
      C1=A1*B1+A2*B2
      C1=C1/TEMP
      C2=B1*A2-A1*B2
      C2=C2/TEMP
      RETURN
      END
      SUBROUTINE HSINX(ARG,X)
      A=EXP(X)
      B=EXP(-X)
      A=A-B
      ARG=.5*A
      RETURN
      END
      SUBROUTINE HCOSX(ARG,X)
      A=EXP(X)
      B=EXP(-X)
      A=A+B
      ARG=.5*A
      RETURN
      END
```

```
      SUBROUTINE ANGL(C,A,B)
      DATA PI/3.1415926/
      C=ABS(B/A)
      C=ATAN(C)
      IF (A.GT.0.) GO TO 5
      IA=1
      GO TO 7
5     IA=0
7     IF (B.GT.0.) GO TO 10
      IB=2
      GO TO 15
10    IB=0
15    IA=IA+IB+1
      GO TO (35,30,25,20),IA
20    C=C-PI
      GO TO 35
25    C=-C
      GO TO 35
30    C=PI-C
35    RETURN
      END
      SUBROUTINE  CALZIN(AZIN1,BZIN1,AZRN1,BZRN1,AZIN2,BZIN2,AN1,DI1,
     1BTN1)
      TEMP=AN1*DI1
      CALL HCOSX(ARG1,TEMP)
      CALL HSINX(ARG2,TEMP)
      TEMP=BTN1*DI1
      CSBI1=COS(TEMP)
      SNBI1=SIN(TEMP)
      ZR=0.
      CALL CMPMP(TEM1,TEM2,AZIN2,BZIN2,ARG1,ZR)
      CALL CMPMP(TEM3,TEM4,AZRN1,BZRN1,ARG2,ZR)
      CALL CMPMP(TEM5,TEM6,AZIN2,BZIN2,ARG2,ZR)
      CALL CMPMP(TEM7,TEM8,AZRN1,BZRN1,ARG1,ZR)
      A1=TEM1+TEM3
      B1=TEM2+TEM4
      A2=TEM5+TEM7
      B2=TEM6+TEM8
      CALL CMPMP(TEM1,TEM2,A1,B1,CSBI1,ZR)
      CALL CMPMP(TEM5,TEM6,A2,B2,CSBI1,ZR)
      CALL CMPMP(TEM7,TEM8,A1,B1,ZR,SNBI1)
      CALL CMPMP(TEM3,TEM4,A2,B2,ZR,SNBI1)
      TEM3=TEM3+TEM1
      TEM4=TEM4+TEM2
      TEM7=TEM7+TEM5
      TEM8=TEM8+TEM6
      CALL CMPDV(TEM1,TEM2,TEM3,TEM4,TEM7,TEM8)
      CALL CMPMP(AZIN1,BZIN1,TEM1,TEM2,AZRN1,BZRN1)
      RETURN
      END
      SUBROUTINE ZEBRA(C1,C2,A1,A2,B1,B2)
      D1=1.
      D2=0.
```

```
CALL CMPDV(ARG1,ARG2,D1,D2,A1,A2)
CALL CMPDV(ARG3,ARG4,D1,D2,B1,B2)
ARG1=ARG1+ARG3
ARG2=ARG2+ARG4
CALL CMPDV(C1,C2,D1,D2,ARG1,ARG2)
RETURN
END
```

Vita

PII Redacted

Mark S. Briski [redacted] the son of Mathew and Dorothy Briski. He graduated from Elgin High School in Elgin, Illinois, in 1965. He enlisted in the Air Force in April of 1974 and was awarded an AFROTC scholarship in 1975 to attend the Illinois Institute of Technology. Upon graduation he was awarded a Bachelor of Science degree in Mechanical-Aerospace Engineering and was commissioned into the Air Force Reserve. In February of 1980 he entered active duty and was assigned to the Foreign Technology Division at Wright-Patterson AFB, Ohio. He was assigned to the Air Force Institute of Technology in June 1982.

Permanent Address: [redacted]

PII Redacted

13/83

REPORT DOCUMENTATION PAGE

1a. REPORT SECURITY CLASSIFICATION UNCLASSIFIED	1b. RESTRICTIVE MARKINGS
2a. SECURITY CLASSIFICATION AUTHORITY	3. DISTRIBUTION/AVAILABILITY OF REPORT Approved for public release; distribution unlimited
2b. DECLASSIFICATION/DOWNGRADING SCHEDULE	
4. PERFORMING ORGANIZATION REPORT NUMBER(S) AFIT/GAE/AA/83D-2	5. MONITORING ORGANIZATION REPORT NUMBER(S)
6a. NAME OF PERFORMING ORGANIZATION School of Engineering 6b. OFFICE SYMBOL (If applicable) AFIT/ENY	7a. NAME OF MONITORING ORGANIZATION
6c. ADDRESS (City, State and ZIP Code) Air Force Institute of Technology Wright-Patterson AFB, OH 45433	7b. ADDRESS (City, State and ZIP Code)
8a. NAME OF FUNDING/SPONSORING ORGANIZATION Flight Dynamics Laboratory 8b. OFFICE SYMBOL (If applicable) AFWAL/FIGL	9. PROCUREMENT INSTRUMENT IDENTIFICATION NUMBER
8c. ADDRESS (City, State and ZIP Code) Flight Dynamics Laboratory AFWAL/FIGL Wright-Patterson AFB, OH 45433	10. SOURCE OF FUNDING NOS. PROGRAM ELEMENT NO. / PROJECT NO. / TASK NO. / WORK UNIT NO.
11. TITLE (Include Security Classification) See Box 19	

12. PERSONAL AUTHOR(S)
Mark S. Briski, B.S., 1 LT., USAF

13a. TYPE OF REPORT	13b. TIME COVERED	14. DATE OF REPORT (Yr., Mo., Day)	15. PAGE COUNT
MS Thesis	FROM ______ TO ______	1983 December	81

16. SUPPLEMENTARY NOTATION

3 JAN 1984 Approved for public release: IAW AFR 190-17.
LYNN E. WOLAVER
Dean for Research and Professional Development
Air Force Institute of Technology (ATC)
Wright-Patterson AFB OH 45433

17. COSATI CODES			18. SUBJECT TERMS (Continue on reverse if necessary and identify by block number)
FIELD	GROUP	SUB. GR.	Frequency Response, Fluid Transmission Lines, Turbulent Mean Flow
20	04		

19. ABSTRACT (Continue on reverse if necessary and identify by block number)

Title: THE EFFECTS OF MEAN FLOW ON THE DYNAMIC CHARACTERISTICS OF FLUID TRANSMISSION LINES

Thesis Chairman: Dr. Milton E. Franke

20. DISTRIBUTION/AVAILABILITY OF ABSTRACT UNCLASSIFIED/UNLIMITED ☒ SAME AS RPT. ☐ DTIC USERS ☐	21. ABSTRACT SECURITY CLASSIFICATION UNCLASSIFIED

22a. NAME OF RESPONSIBLE INDIVIDUAL	22b. TELEPHONE NUMBER (Include Area Code)	22c. OFFICE SYMBOL
Dr. Milton E. Franke	(513) 255-2362	AFIT/ENY

Theoretical predictions of the small signal frequency response of round pneumatic transmission lines with turbulent mean flow were compared with experimental results. The frequency response curves were found for lines varying in length from 24 to 36 in. with inside diameters of 0.195, 0.119, and 0.041 in. The lines were tested at Reynolds numbers of 2000, 5000, and 10000.

Theoretical solutions were obtained using Nichols' equations as modified by Krishnaiyer and Lechner. Solutions were also found using several different modifications of a constant LRC model developed by Moore. The results were mixed: for the 0.195 and 0.119 in. lines the prediction of gain was good but for the 0.041 in. lines the results were poor. The accuracy and applicability of the constant LRC model was explored along with its various modifications. The constant LRC model with the AC resistance showed potential for predicting the gain in fluid transmission lines with turbulent flow. The limitations and applicability of the constant LRC models was studied.